

Calibrating the Early Cretaceous Urho Pterosaur Fauna in Junggar Basin and implications for the evolution of the Jehol Biota

Daran Zheng^{1,†}, Su-Chin Chang^{2,†}, Jahandar Ramezani³, Xing Xu^{4,5}, Honghe Xu¹, He Wang¹, Rui Pei⁴, Yanan Fang¹, Jun Wang⁵, Bo Wang¹, and Haichun Zhang¹

¹State Key Laboratory of Palaeobiology and Stratigraphy, Nanjing Institute of Geology and Palaeontology and Center for Excellence in Life and Palaeoenvironment, Chinese Academy of Sciences, 39 East Beijing Road, Nanjing 210008, China

²Department of Earth Sciences, The University of Hong Kong, Pokfulam Road, Hong Kong 999077, China

³Department of Earth, Atmospheric and Planetary Sciences, Massachusetts Institute of Technology, 77 Massachusetts Avenue, Cambridge, Massachusetts 02139, USA

⁴Key Laboratory of Vertebrate Evolution and Human Origins, Institute of Vertebrate Paleontology and Paleoanthropology (IVPP), Chinese Academy of Sciences, Beijing 100044, China

⁵School of Earth Sciences, Yunnan University, Kunming 650500, China

ABSTRACT

Over the past decades, abundant and well-preserved vertebrate fossils, known as the Urho Pterosaur Fauna, have been recovered from the Lower Cretaceous Tugulu Group in Junggar Basin, Xinjiang, NW China. Excavated materials belong to pterosaur, plesiosaur, dinosaur, crocodylomorph, and turtle taxa. As such, they provide key insights into the evolutionary history of several critical vertebrate groups in the Early Cretaceous. The Junggar assemblages have been interpreted as belonging to the Jehol Biota *sensu lato*, representing its northwesternmost known geographic extent. This research presents a new chemical abrasion–isotope dilution–thermal ionization mass spectrometry U–Pb age of 135.2 ± 0.9 Ma (2σ internal error) from a tuffaceous bed stratigraphically below the fauna-bearing layers, indicating a Valanginian maximum age for the Urho fauna. Combined with available biostratigraphic data, the results bear several important paleobiologic implications for the Early Cretaceous vertebrates. First, the *Dsungaripterus* pterosaur and *Psittacosaurus* ornithischian fauna appear to have emerged earlier than previously believed. Second, the data suggest that the oldest carcharodontosaurids in Asia appeared during the Valanginian Stage and extend the age range of basal coelurosaurs and basal crocodyliforms. Our

results do not support the notion of the Jehol Biota *sensu lato* migrating as far west as the Junggar Basin in their later stages. The new information calls into question the temporal and spatial bases for the conventional, three-stage evolutionary theory of the Jehol Biota.

INTRODUCTION

Lower Cretaceous strata in eastern Asia primarily consist of terrestrial sediments deposited in inland basins, which preserve abundant and diverse fossils referred to as the Jehol Biota (e.g., Chen, 1999; Zhou et al., 2003, 2021; Xu et al., 2020). This exceptionally well-preserved middle Early Cretaceous (ca. 135–115 Ma) lagerstätte centered geographically in northeast China contains feathered dinosaurs, early birds, pterosaurs, mammals, invertebrates, and flowering plants (Zhou et al., 2003, 2021; Xu et al., 2020; Zheng et al., 2021). The Jehol Biota *sensu lato* is thought to appear in Junggar Basin (Fig. 1), where it generally includes the pterosaur *Dsungaripterus* and the dinosaur *Psittacosaurus* but lacks typical Jehol elements like *Ephemeropsis trisetalis* (insect), *Eosestheria* (clam shrimp), and *Lycoptera* (fish) (the “EEL” assemblage; Chen, 1999). However, the EEL assemblage is found in the Hexi Corridor to the southeast (Fig. 1; Zheng et al., 2021). This raises questions about whether the Junggar Basin fell within the migrational area of the late-stage Jehol Biota.

The Urho Pterosaur Fauna is an important vertebrate fauna in central Asia. It contains abundant fossils, including the pterosaurians *Dsungaripterus weii* and *Noriopterus complicidens*, the ornithischians *Psittacosaurus xinjiangensis*

and *Wuerhosaurus homheni*, the saurischians *Tugulusaurus faciles*, *Xinjiangovenator parvus*, *Kelmaysaurus petrolicus*, and cf. *Asiatosaurus mongoliensis*, the protosuchian *Edentosuchus tienshanensis*, the plesiosaur *Sinopliosaurus weiyuanensis*, and the turtles *Xinjiangchelys* sp. and *Ordosemys brinkmania* (Table S1¹). *Dsungaripterus* and *Psittacosaurus* represent the predominant organisms of the Urho Pterosaur Fauna (Young, 1964, 1973). Besides the Urho Pterosaur Fauna in NW Junggar Basin, the Tugulu Group in the southern and eastern parts of Junggar Basin contains fossils of dsungaripterid pterosaurs (Maisch et al., 2004; Augustin et al., 2021, 2022a, 2022b), siyueichthyid fish (Su, 1980), and diverse turtles (Brinkman et al., 2001; Matzke and Maisch, 2004; Maisch et al., 2003). In Hami Basin (Fig. 2A), the Tugulu Group hosts exceptionally well-preserved skeleton and egg fossils belonging to the pterosaur *Hamipterus tianshanensis*, which have been key to understanding the pterosaur’s reproduction and nesting behavior (Wang et al., 2014, 2017).

Although Tugulu Group strata in Junggar and Hami Basins contain one of the most diverse vertebrate assemblages in central Asia, no reliable age constraints exist for these units. The absence of absolute age data limits understanding of this fauna in an evolutionary context. Here, we report a new U–Pb zircon age obtained from a tuffaceous sample collected below the vertebrate fossil-bearing layers found in and around the Urho district of NW Junggar Basin. This radioisotopic age refines interpretations of the evolution of the Urho Pterosaur Fauna in NW China and calls for revisions to the prevailing three-stage evolutionary theory for the Jehol Biota *sensu lato*.

Su-Chin Chang  <https://orcid.org/0000-0002-5232-5152>

[†]dranzheng@gmail.com; suchin@hku.hk

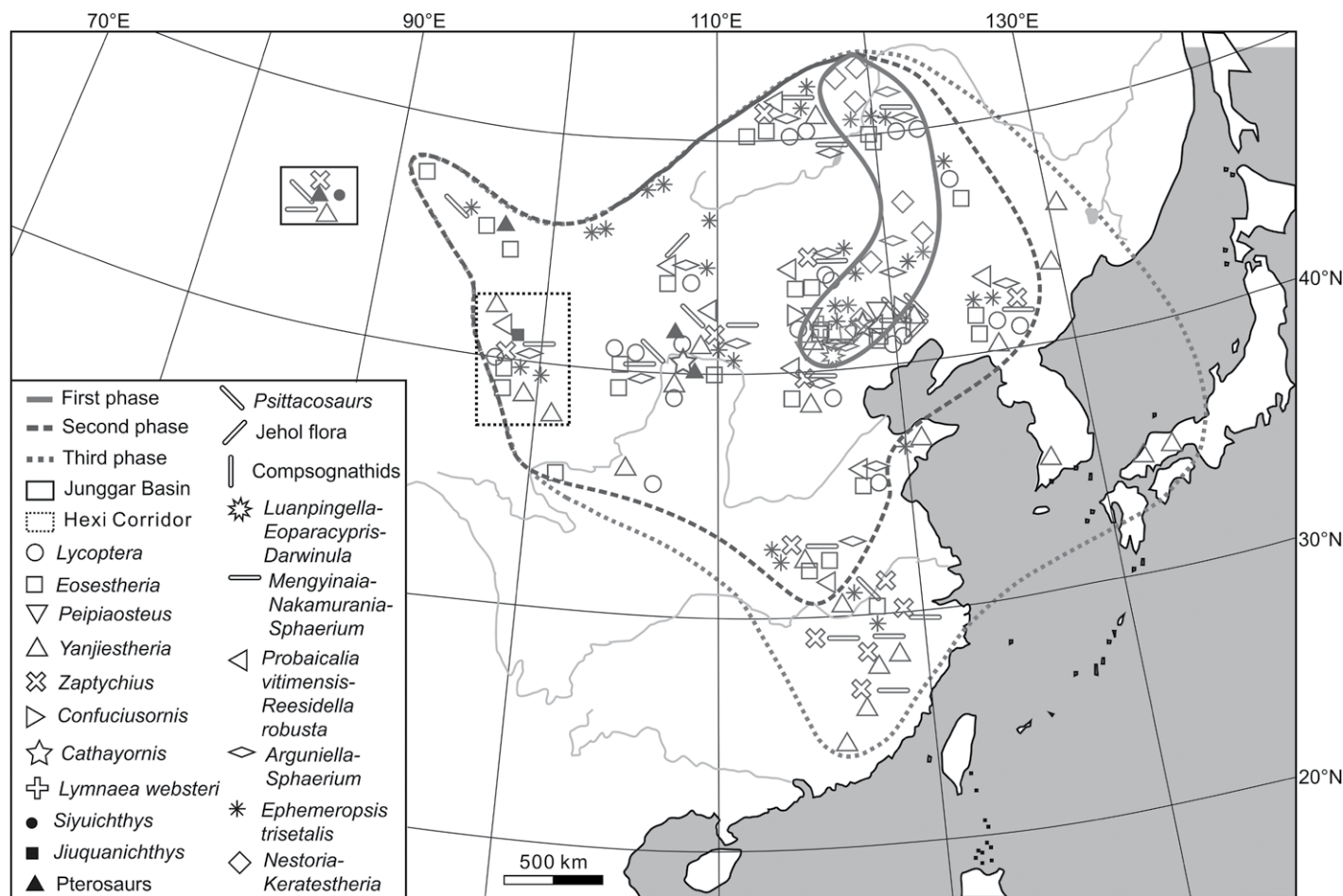


Figure 1. Reshaped three-stage evolution and migration map for the Jehol Biota sensu lato (revised from Chen, 1999).

GEOLOGICAL BACKGROUND

The Junggar Basin is a large continental basin with a history of Permian to Quaternary sedimentation (Eberth et al., 2001), units of which crop out throughout the Xinjiang Uygur Autonomous Region, NW China (Fig. 2A). The basin includes successions of Mesozoic sediments that can reach thicknesses up to 6 km. Cretaceous strata of the Junggar Basin indicate a complex fluvial-deltaic-lacustrine environment (Eberth et al., 2001). Early Cretaceous sediments within the Tugulu Group are well exposed along the northern and southern rims of Junggar Basin. These outcrops host abundant pterosaur, plesiosaur, dinosaur, crocodylomorph, and turtle fossils (Fig. 2B; see Table S1). Within the southern Junggar Basin proper, the Tugulu Group consists (in ascending order) of the Qingshuihe, Hutubihe, Shengjinkou, and Lianmuqin Formations, but the Qingshuihe Formation does not occur in the NW Junggar Basin (Zhao, 1980). In the NW Junggar Basin, vertebrate fossil-bearing

outcrops occur at the Urho and Delunshan localities. Respectively, these localities host prominent examples of the *Dsungaripterus* and *Psittacosaurus* fauna (Fig. 2B). The occurrence of *Dsungaripterus* and *Psittacosaurus* in both sections suggests a correlation between the two units. Compositional differences between the two faunas have been interpreted in terms of depositional facies and preservation bias (Zhao, 1980).

In Urho, vertebrate fossils primarily occur in sandstone and mudstone horizons of the Lianmuqin Formation to the southeast, near Alice Lake. Track fossils occur in a sandstone horizon of the Hutubihe Formation near Huangyangquan reservoir (Fig. 2C). A distinct, white tuffaceous siltstone (0.2 m thick; Fig. 3), lying ~30 m below the vertebrate-bearing layers, serves as a marker horizon that separates the Shengjinkou and Lianmuqin Formations in the NW Junggar Basin. A 5 kg sample (sample W-1) from this tuffaceous bed (Fig. 3) was collected from the Jiamuhe outcrop near Urho (46°1'55"N, 85°38'5"E) for U-Pb zircon geochronology. The Supplemental

Material¹ provides additional information about this unit and the tuffaceous bed.

MATERIALS AND METHODS

U-Pb Geochronology

In total, 100 inclusion-free zircon grains from the Jiamuhe section tuffaceous sample W-1 were

¹Supplemental Material. Supplemental Text S1: Stratigraphic information, U-Pb geochronology by LA-MC-ICP-MS, and U-Pb geochronology by CA-ID-TIMS. Figure S1: Cathodoluminescent images of zircons from sample W-1 with youngest ages analyzed by LA-MC-ICP-MS U-Pb dating. Figure S2: Rank order plot of LA-MC-ICP-MS U-Pb ages for youngest zircon subpopulations from sample W-1. Table S1: Vertebrate and trace fossils from the Tugulu Group of Junggar Basin. Table S2: LA-MC-ICP-MS U-Pb analytical results for standard zircons and sample W-1. Table S3: CA-ID-TIMS U-Pb analytical results for sample W-1. Please visit <https://doi.org/10.1130/GSAB.S.22250917> to access the supplemental material, and contact editing@geosociety.org with any questions.

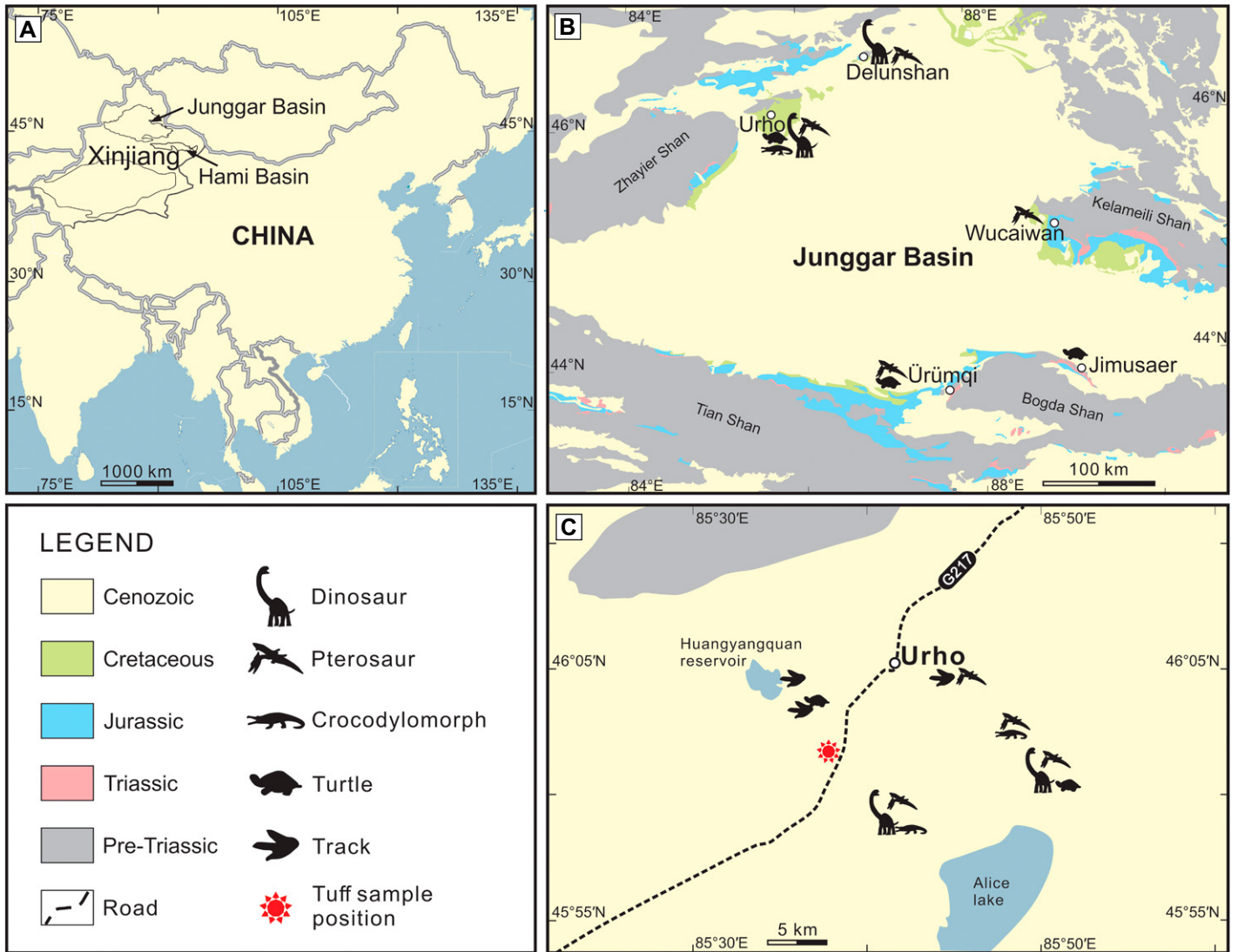


Figure 2. Distribution of Early Cretaceous vertebrate fossils within Junggar Basin. (A) Map showing the position of the Junggar Basin in Xinjiang, NW China. (B) Distribution of vertebrate fossils in the Junggar Basin. (C) Distribution of vertebrate fossils around Urho, NW Junggar Basin.

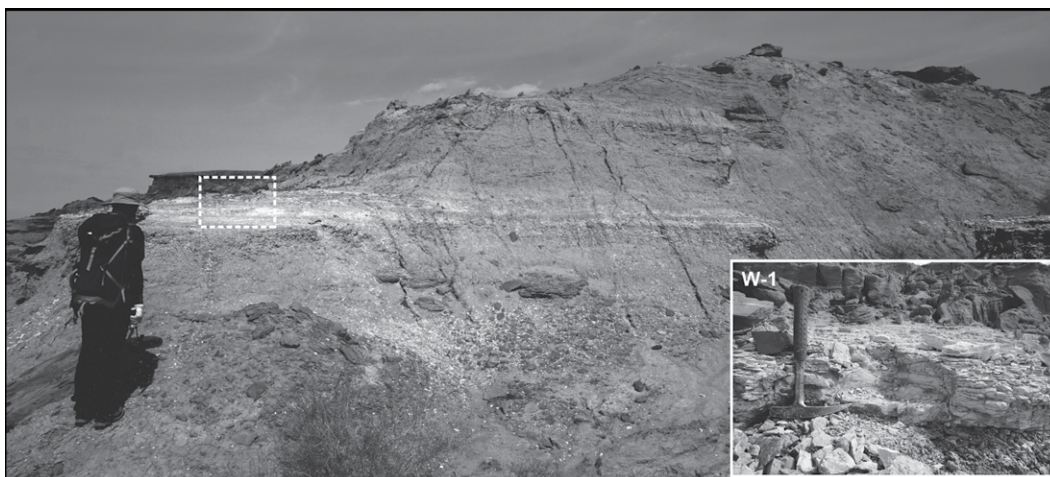


Figure 3. Images of tuffaceous sample W-1 as it occurs within the Jiamuhe outcrop, Urho, NW Junggar Basin.

mounted in epoxy resin, polished to expose grains midsection, and imaged by cathodoluminescence (CL) to document grain morphologies and internal zoning (Fig. S1). Zircons were analyzed using the in situ laser ablation–multicollector–inductively coupled plasma–mass spectrometry (LA-MC-ICP-MS) technique at the Department of Earth Sciences, University of Hong Kong. High-precision chemical abrasion–isotope dilution–thermal ionization mass spectrometry (CA-ID-TIMS) analyses were conducted on carefully selected zircons at the Massachusetts Institute of Technology Isotope Laboratory to help validate age accuracy. Analytical details are given in the Supplemental Material, and Table S2 lists U–Pb data results.

RESULTS

The zircon grains separated from sample W-1 were small (35–70 μm in length) but exhibited uniform, euhedral and equant morphologies with typical oscillatory zoning patterns of magmatic zircons. Sharply faceted crystals suggest minimal sedimentary transport prior to the deposition of the tuffaceous sample. Twenty LA-MC-ICP-MS analyses yielded $^{206}\text{Pb}/^{238}\text{U}$ dates that ranged from 762 Ma to 132 Ma, indicating the presence of a detrital zircon component (Fig. 4A; see Table S2). A subpopulation of nine effectively concordant analyses (concordance $\geq 95\%$) from the young end of the age spectrum ranged in $^{206}\text{Pb}/^{238}\text{U}$ dates between 135.7 ± 1.0 Ma and 134.4 ± 1.8 Ma (Fig. 4A) and produced a weighted mean age of $135.2 \pm 0.5/0.6$ Ma (mean square of weighted deviates [MSWD] = 0.4; 2σ uncertainty; Fig. S2). The seven older ages (762–278 Ma) from the sample are interpreted as detrital or xenocrystic. Five carefully selected single zircons (sharply faceted, unbroken, bipy-

ramids) analyzed independently by CA-ID-TIMS yielded a significantly narrower $^{206}\text{Pb}/^{238}\text{U}$ age range of 141.51 ± 0.87 Ma to 135.21 ± 0.92 Ma (Fig. 4B; Table S3). The ~ 6 m.y. scatter in the analyses prevented the calculation of a statistically meaningful weighted mean age.

DISCUSSION

Age of the Urho Tuffaceous Siltstone

The presence of zircons of pre-Cretaceous age, along with the absence of additional tuffaceous beds from the Tugulu Group that would allow an age-superposition test, complicates the interpretation of the measured U–Pb dates of this study. While the youngest zircon analyses by LA-MC-ICP-MS converge at ca. 135 Ma, the higher precision of the CA-ID-TIMS analyses (averaged ± 0.73 m.y.) reveals data scatter beyond the age resolution of the LA-MC-ICP-MS method (averaged ± 1.6 m.y.). Nevertheless, the sampled bed at the Jiamuhe section has all the characteristics of a tuffaceous siltstone (see Supplemental Materials), and the recovered zircon population appears to be morphologically uniform with no visible signs of rounding due to sedimentary transportation. These factors suggest that the older zircons were either antecrysts or originated from country rocks at the site of pyroclastic eruption. Therefore, we interpret the $^{206}\text{Pb}/^{238}\text{U}$ date of the youngest CA-ID-TIMS analysis at 135.21 ± 0.92 Ma, which overlaps with the weighted mean age of the nine youngest LA-MC-ICP-MS analyses (135.2 ± 0.6 Ma), as a reliable estimate for the age of zircon crystallization in the Urho tuffaceous sample. The latter serves as the best available maximum constraint for the depositional age of the sample and associated strata at this time.

Biostratigraphic Age for the Tugulu Group

Invertebrate fossils from the Tugulu Group of the southern Junggar Basin were used to interpret a biostratigraphic age for the unit. Clam shrimp, ostracod, charophyte, and sporopollen fossil assemblages have been cited as evidence of an Early Cretaceous age for the Tugulu Group (Chen and Wei, 1985; Yu et al., 1986). The Qingshuihe Formation was interpreted as Berriasian in age based on clam shrimp, ostracod, and sporopollen fossils (Wang et al., 2012; Wang, 2013). Clam shrimp fossils dominated by *Nestoria* (Chen and Wei, 1985; Wang, 2013) are slightly younger than the *Nestoria-Keratostheria* assemblage found in the uppermost Jurassic of North China and Russia and are thus categorized as Berriasian (Wang et al., 2012). The *Lygodiumsporites-Densoisporites-Cicatricosisporites-Protoconiferus* sporopollen assemblage from the Qingshuihe Formation carries a similar age interpretation (Wang et al., 2012). The Hutubihe Formation contains abundant clam shrimp fossils belonging to *Ortheastheria intermedia*. These also occur in the Lower Cretaceous Shouchang Formation of west Zhejiang, SE China (Chen and Wei, 1985; Chen, 2003). The Hutubihe Formation also contains the sporopollen assemblage *Toroisporites-Densoisporites-Classopollis-Piceapollenites*, indicating a Valanginian age (Yu et al., 1986). The Shengjinkou Formation contains the clam shrimp fossils *Ortheastheria* sp., *Yanjiertheria* sp., and *Linhaiella xiyuensis* (Chen, 2003), as well as the sporopollen assemblage *Lygodiumsporites-Coneavissisporites-Classopollis-Piceapollenites*, but it lacks angiosperm pollens (Yu et al., 1986). Along with the siyuichthyid fish (Su, 1980; Eberth et al., 2001), these fossils indicate an Early Cretaceous biostratigraphic age. Our ca. 135.2 Ma U–Pb age

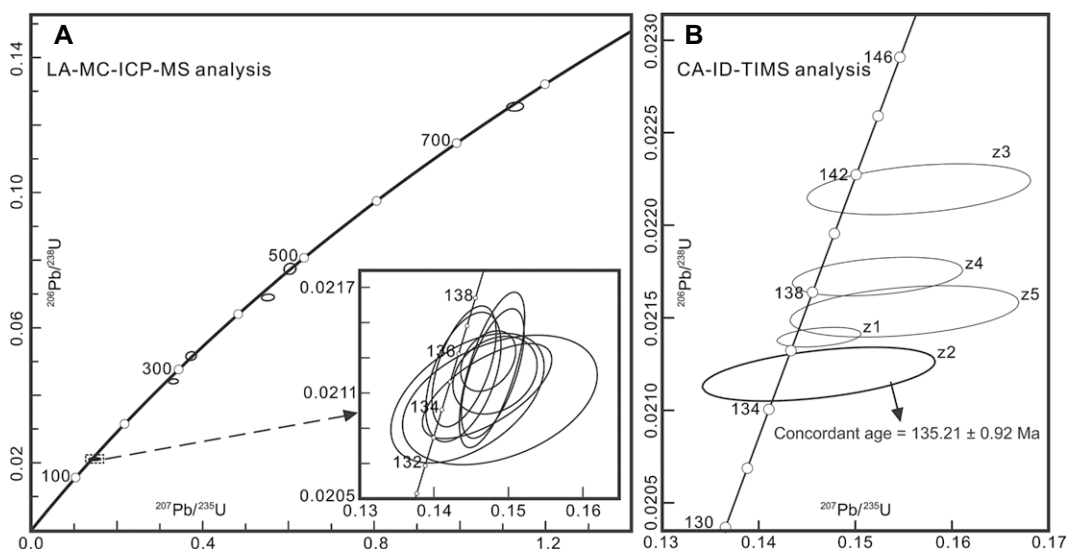


Figure 4. U–Pb concordia plots of zircons analyzed from sample W-1. (A) Laser ablation–multicollector–inductively coupled plasma–mass spectrometry (LA-MC-ICP-MS) analysis. (B) Chemical abrasion–isotope dilution–thermal ionization mass spectrometry (CA-ID-TIMS) analysis. Age uncertainties are given at the 2σ level. See Table S2 for U–Pb data (see text footnote 1).

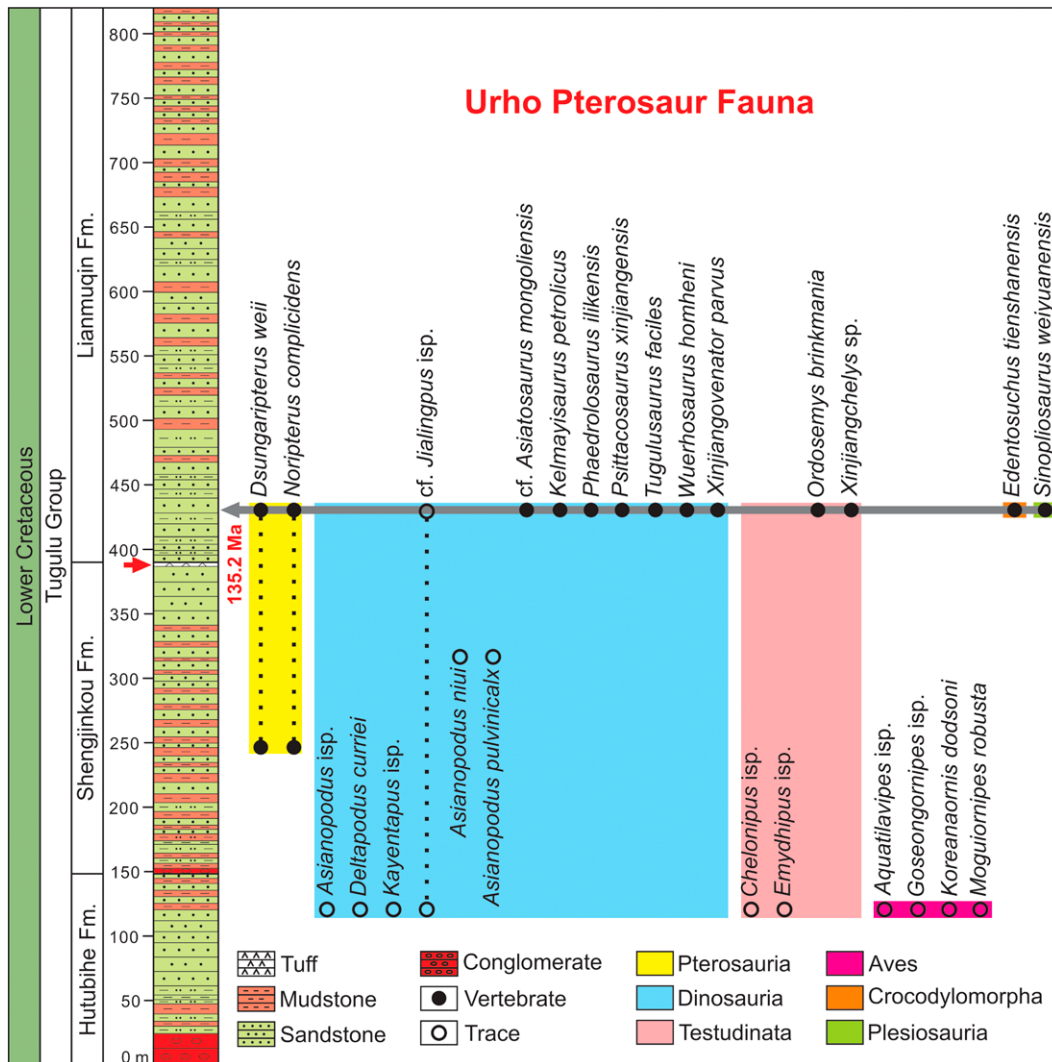


Figure 5. Stratigraphy and vertebrate fauna of the Tugulu Group within the Jiamuhe outcrop. Stratigraphic column is after Zhao (1980), and fossil data are from Table S1 (see text footnote 1).

places the upper Shengjinkou Formation within the Valanginian Stage.

The Lianmuqin Formation contains the clam shrimp fossil *Cratostracus* sp., which also occurs in the Guantou Formation (Aptian) of Zhejiang (Chen, 1994). Sporopollen from the Lianmuqin Formation includes the *Cicatricosisporites-Interulobites-Classopollis-Tricolpites* assemblage along with occasional angiosperm pollens belonging to *Tricolpites*, *Clavatipollenites*, and *Aestropollis* (Yu et al., 1986). This assemblage closely resembles that found within the Upper Hekou Formation in Qinghai, a unit interpreted to be Aptian–Albian in age (Ji, 1994). The angiosperm pollens listed above also occur in the Zhonggou Formation of Jiuquan Basin, which is interpreted as Albian in age (Zhang et al., 2015). The paleontological evidence thus indicates an Aptian–Albian age for the Lianmuqin Formation of the southern Junggar Basin. This age represents a maximum depositional age for the layers containing vertebrate fossils in the lower

Lianmuqin Formation of Urho (Zhao, 1980). However, our isotopic age from the top of the Shengjinkou Formation indicates that the Lianmuqin Formation could have been deposited as early as the Valanginian. The Tugulu Group thus formed during the Early Cretaceous. While our maximum age estimate does not preclude a post-Valanginian depositional age, the combination of radioisotopic and biostratigraphic constraints supports the following age model for the group: the Qingshuihe Formation as Berriasian, the Hutubihe and Shengjinkou Formations as Valanginian, and the Lianmuqin Formation as Valanginian to Albian.

Implications for the Evolution of the *Dsungaripterus* Pterosaur Fauna

Pterosaurs excavated from Junggar Basin belong to the Dsungaripteridae, primarily the species *Dsungaripterus weii* and *Noripterus complicidens* in northern Junggar Basin, as well

as the much rarer *Lonchognathosaurus acutirostris* in southern Junggar Basin (Fig. 5; Young, 1964; Buffetaut, 1996; Maisch et al., 2004; Li and Ji, 2010; Hone et al., 2018; Augustin et al., 2021). *Dsungaripterus* and *Noripterus* probably coexisted over a protracted time frame, and both occur in the Shengjinkou and Lianmuqin Formations around Urho (Zhao, 1980). *Dsungaripterus* may have fed on shelled invertebrates in shallow lakes (Chen et al., 2020). *Noripterus* meanwhile fed on fish in deeper lacustrine environments (Lü et al., 2009). Dsungaripteridae fossils also appear in western Mongolia, South America, and Europe (Lü et al., 2009; Martill et al., 2000; Hone et al., 2018). In western Mongolia, both *Dsungaripterus* and *Noripterus* occur in the lower part of the Lower Cretaceous Tsagan Tsab Formation (Berriasian–Valanginian; Lukashovich and Przhiboro, 2015), indicating a connected ecospace between western Mongolia and Xinjiang (Lü et al., 2009). The age constraints (post–early Valanginian) for the pterosaur fauna

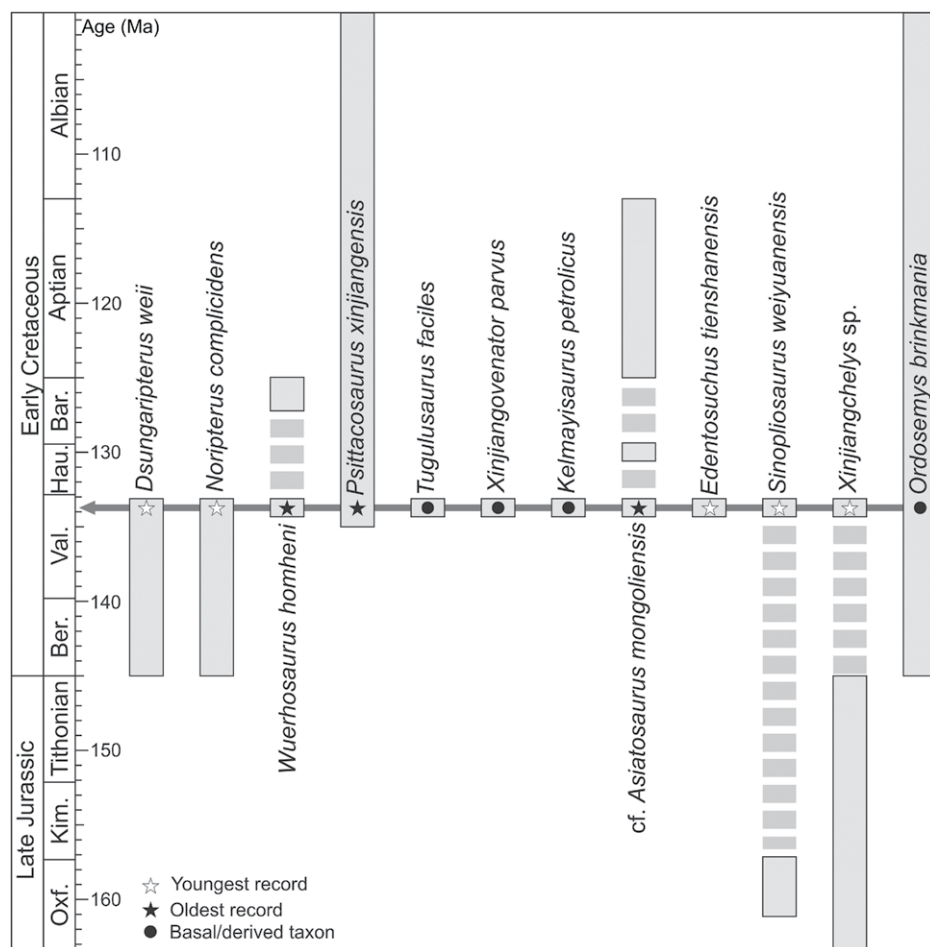


Figure 6. Evolution of the Urho Pterosaur Fauna in NW Junggar Basin. Extension of taxa into the Late Jurassic and Early Cretaceous was interpreted at the genera level. Age abbreviations: Oxf.—Oxfordian, Kim.—Kimmeridgian, Ber.—Berriasian, Val.—Valanginian, Hau.—Hauterivian, Bar.—Barremian.

in this study fall within the interpreted age range of the vertebrate assemblage in western Mongolia (Fig. 6).

The Xinjiang dinosaurs include ornithischians *Psittacosaurus xinjiangensis* and *Wuerhosaurus homheni* and saurischians *Tugulusaurus faciles*, *Xinjiangovenator parvus*, *Kelmaysaurus petrolicus*, and *cf. Asiatosaurus mongoliensis* (Fig. 5; Dong, 1973; Zhao, 1980; Sereno and Chao, 1988; Brinkman et al., 2001; Rauhut and Xu, 2005; Lucas, 2006). Among them, *Psittacosaurus xinjiangensis* fossils occur at the Urho and Delunshan localities (Sereno and Chao, 1988; Brinkman et al., 2001). *Psittacosaurus* had a relatively wide geographic distribution throughout East Asia. This organism's fossils occur in Barremian to Albian units of northern China (Xinjiang, Inner Mongolia, Gansu, Ningxia, Liaoning, Hebei, and Shandong Provinces), Mongolia, Russia, Thailand, and potentially the Japanese islands (Lucas, 2006).

The lowermost *Psittacosaurus*-bearing horizon recorded in the Yixian Formation in northeast China is Hauterivian in age based on $^{40}\text{Ar}/^{39}\text{Ar}$ and U-Pb geochronology (ca. 126–122 Ma for the Yixian Formation; He et al., 2006; Chang et al., 2009; Zhong et al., 2021; Li et al., 2022), but an even lower horizon in the Dabeigou Formation (ca. 135–129 Ma; Zhang et al., 2022) is presently under investigation (Xu Xing, personal commun.). The appearance of *Psittacosaurus* fossils in NW Junggar Basin represents one of the oldest records of this genus (Fig. 6). Fossils belonging to the ornithischian *Wuerhosaurus* also appear in the Lower Cretaceous Ejinhor Formation of the Ordos Basin, Inner Mongolia, and have been referred to their own species *Wuerhosaurus ordosensis* (Dong, 1993). The Ejinhor Formation was interpreted as late Barremian in age (Cuenca-Bescós and Canudo, 2003). The *Wuerhosaurus* fossils found in late Valanginian strata thus appear to be much older

than those found in the Inner Mongolian units. *Tugulusaurus* is among the most basal coelurosaurians, but its fossils occur in the highest (youngest) horizon. *Xinjiangovenator* represents another derived coelurosaurian (Rauhut and Xu, 2005). The coelurosaurians from the Urho locality indicate degrees of endemism among the theropod fauna of Central Asia rather than mingling of European and East Asian faunas (Rauhut and Xu, 2005). *Kelmaysaurus petrolicus* is a basal carcharodontosaurid and the second known member of the family in Asia. Another carcharodontosaurid, *Chilantaisaurus maortuensis*, has been excavated from lower Upper Cretaceous strata (ca. 92 Ma; Turonian) of Inner Mongolia (Kobayashi and Lü, 2003; Brusatte et al., 2009). Our new age constraint places the first appearance of large-bodied predators in Asia within the late Valanginian. *Asiatosaurus mongoliensis* fossils were initially discovered in Lower Cretaceous units around Red Mesa, Mongolia (Osborn, 1924), interpreted to be ca. 130.0 Ma (Conrad and Daza, 2015). *A. mongoliensis* was later found in Lower Cretaceous units of Two Volcanoes, Mongolia, which are interpreted to be Aptian in age (Ksepka et al., 2005). The age reported here renders the appearance of *A. mongoliensis* earlier than the example from Red Mesa, Mongolia.

In Junggar Basin, a sole basal protosuchian, *Edentosuchus tienshanensis*, from the Lianmuqin Formation of Urho (Young, 1973; Li, 1985; Pol et al., 2004), represents the youngest-known protosuchid crocodylomorph (Wings et al., 2010). *Edentosuchus* was considered to be a sister taxon of an unnamed Lower Jurassic Kayenta taxon from Arizona, southwestern United States (Pol et al., 2004). Together, these represent the sister group to the clade that includes *Hemiprotosuchus leali* (Upper Triassic of Argentina; Bonaparte, 1969) and *Protosuchus richardsoni* (Lower Jurassic of Arizona; Brown, 1933). The correlation with the latter Late Triassic to Early Jurassic taxa supports the interpretation that basal crocodyliformes survived much longer in Central Asia than previously believed (Pol et al., 2004). The results reported here and correlations would extend the upper age range of this basal crocodyliform to at least the Valanginian Stage. The result also suggests its adaptation to the hot and seasonal arid climate of the NW Junggar Basin (Eberth et al., 2001; Wings et al., 2010). A plesiosaur, *Sinopliosaurus weiyuanensis*, was also excavated from the Lianmuqin Formation (Young, 1973). *S. weiyuanensis* was initially recorded from the Upper Jurassic Shaximiao Formation in Sichuan, southern China (Young, 1944), dated at ca. 159 ± 2 Ma (Oxfordian; Wang et al., 2018). Our new age extends the age range of *S. weiyuanensis* to the Early Cretaceous.

CONCLUSIONS

The Early Cretaceous Urho Pterosaur Fauna excavated from Junggar Basin contains abundant vertebrate fossils, including pterosaur, plesiosaur, dinosaur, crocodylomorph, and turtle taxa. This biota was believed to be related to the well-known Jehol Biota, representing its northwesternmost extent in eastern Asia, although characteristic elements of the Jehol Biota sensu lato (“EEL” assemblage) are absent from Junggar Basin. A U-Pb zircon age of 135.2 ± 0.9 Ma for an isolated tuffaceous sample from the Jiamuhe section in northwest Junggar Basin and relevant biostratigraphic constraints support a Valanginian age for the fauna. Our age model indicates that *Dsungaripterus* fossils and the oldest carcharodontosaurids in Asia appeared during the Valanginian Stage, providing significant input for hypotheses related to the evolution of key Cretaceous vertebrates. Our study further suggests that the Jehol Biota sensu lato did not reach as far west as the Junggar Basin in its later stages, which necessitates revisions to the conventional evolutionary theory of the Jehol Biota in space and time.

ACKNOWLEDGMENTS

This research was supported by the National Natural Science Foundation of China (42125201, 42288201), HKU Seed Funding Program for Basic Research (202111159061), the Strategic Priority Research Program of the Chinese Academy of Sciences (XDA19050101, XDB26000000), the Second Tibetan Plateau Scientific Expedition and Research (2019QZKK0706), and the Chinese Academy of Sciences (E221020002). We thank Qingzhu Yin for constructive comments that improved this manuscript. Felix Augustin and two anonymous reviewers are acknowledged for their constructive feedback.

REFERENCES CITED

- Augustin, F.J., Matzke, A.T., Maisch, M.W., and Pflretzschner, H.-U., 2021, New information on *Lonchognathosaurus* (Pterosauria: Dsungaripteridae) from the Lower Cretaceous of the southern Junggar Basin (NW China): *Cretaceous Research*, v. 124, <https://doi.org/10.1016/j.cretres.2021.104808>.
- Augustin, F.J., Matzke, A.T., Maisch, M.W., and Csiki-Sava, Z., 2022a, Pterosaur remains from the Lower Cretaceous Lianmuxin Formation (upper Tugulu Group) of the southern Junggar Basin (NW China): *Historical Biology*, v. 34, p. 312–321, <https://doi.org/10.1080/08912963.2021.1910819>.
- Augustin, F.J., Matzke, A.T., Maisch, M.W., Kampouridis, P., and Csiki-Sava, Z., 2022b, The first record of pterosaurs from the Lower Cretaceous Hutubei Formation (lower Tugulu Group) of the southern Junggar Basin (NW China)—A glimpse into an unusual ecosystem: *Cretaceous Research*, v. 130, <https://doi.org/10.1016/j.cretres.2021.105066>.
- Bonaparte, J.F., 1969, Dos nuevas ‘faunas’ de reptiles Triasicos de Argentina, in *Gondwana Stratigraphy (IUGS Symposium, Buenos Aires)*, Volume 2: Buenos Aires, Argentina. International Union of Geological Sciences, p. 283–306.
- Brinkman, D.B., and Peng, J., 1993, *Ordosemys leios*, n. gen., n. sp., a new turtle from the Early Cretaceous of

Turtle fossils from the Lower Cretaceous units of the Junggar Basin belong to the derived eucryptodire “Sinemydidae”/“Macrobaenidae” assemblage (Yeh, 1973; Rabi et al., 2010). This assemblage includes *Wuguia efremovi* and *Wuguia hutubeiensis* from the Hutubei Formation, and *Xinjiangchelys* sp., *Ordosemys brinkmania*, cf. *Pantrionychia* indet., *Dracochelys bicuspis*, and *Dracochelys wimani* from the Lianmuqin Formation (Brinkman et al., 2001; Matzke and Maisch, 2004; Maisch et al., 2003, 2004; Danilov and Parham, 2007; Rabi et al., 2010). As such, it represents one of the most diverse Early Cretaceous turtle assemblages in Asia. The assemblage also resembles others that occur around northern China, Mongolia, and the Lake Baikal region of Russia (Rabi et al., 2010). Besides the genera *Xinjiangchelys* and *Ordosemys* recorded outside the Junggar Basin, all other taxa are endemic in the Tugulu Group. *Xinjiangchelys* is the dominant turtle throughout Upper Jurassic strata of Asia, and its appearance in the Lianmuqin Formation represents its last appearance in Asia (Danilov and Parham, 2007; Rabi et al., 2010). *Ordosemys* is distributed in the Lower Cretaceous units of Asia, with occurrences in the Luohandong Formation of Inner Mongolia (Hauterivian–Albian; Brinkman and Peng, 1993), the Yixian Formation of Liaoning (Hauterivian–Aptian; Tong et al., 2004), the Mengyin Formation of Shandong (Berriasian–Valanginian; Li et al., 2019), the Hengtongshan Formation of Jilin (early Aptian; Zhou et al., 2019), and the Khulsangol Formation of Mongolia (Albian; Sukhanov, 2000). The presence of *Ordosemys* fossils in late Valanginian-aged sediments of Urho is consistent with the age range of other units in which other *Ordosemys* fossils occur. In addition to body fossils, hundreds of tracks occur in the Hutubei Formation. These were made by small shorebirds, nonavian dinosaurs, pterosaurs, turtles, and invertebrates (Xing et al., 2014; Li et al., 2020). Such was the diverse animal community within the NW Junggar Basin.

Implications for the Evolution of the Jehol Biota

The Jehol Biota sensu stricto of northeast China occurs in western Liaoning, northern Hebei, and southeast Inner Mongolia provinces, while the Jehol Biota sensu lato defines a much wider area (Fig. 1) that extended northward to Transbaikalia, eastward to Japan, southward to Fujian, and westward to Xinjiang in China (Chen, 1999; Zhou et al., 2003, 2021; Li et al., 2022). This biota has been divided into early, middle, and late evolutionary stages (Chen, 1999; Zhou et al., 2003, 2021), with represen-

tative fossil assemblages respectively appearing in the Dabeigou (ca. 135–129 Ma; Fang et al., 2022; Yu et al., 2022; Zhang et al., 2022), Yixian (ca. 126–122 Ma; Zhong et al., 2021; Li et al., 2022), and Jiufotang (ca. 122–115.5; He et al., 2006; Chang et al., 2009; Zheng et al., 2021) Formations, as well as in correlated strata throughout eastern Asia.

The Junggar Basin has long been considered to be the northwesternmost occurrence of the late Jehol Biota (Chen, 1999; Zhou et al., 2021). Junggar Basin strata contain *Psittacosaurus* (dinosaur), *Siyuichthys* (fish), *Mengyinai-Nakamuraia-Sphaerium* (bivalve), *Yanjiestheria* (clam shrimp), and *Zaptychius* (gastropod) fossils (Chen, 1999). These taxa, however, offer few biostratigraphic constraints. As discussed above, *Psittacosaurus* occurs within Barremian to Albian strata, and materials of the fish fossil *Siyuichthys* show highly localized distributions (Su, 1980). The Early Cretaceous description of the bivalve assemblage requires further investigation and validation (Wei, 1982; Jiang et al., 2007), as well. *Yanjiestheria* appears by the late Dabeigou Formation (ca. 129 Ma; Li et al., 2007), and *Zaptychius* occurs throughout the Lower Cretaceous of China (Pan et al., 2014). In addition to the paucity of cosmopolitan fauna with limited temporal distributions, typical elements of late Jehol Biota, i.e., *Ephemeroptera trisetalis*, *Eosestheria*, and *Lycoptera*, are absent from Junggar Basin. The assemblage thus offers only a few links between the Urho Pterosaur Fauna and the late Jehol Biota. The late Jehol Biota has been dated at ca. 122–115.5 Ma (Zheng et al., 2021), younger than our age model for the Urho Pterosaur Fauna. The age and faunal differences indicate that the latter was distinct from the Jehol Biota and represents an unrelated local fauna inhabiting the Junggar Basin. The typical elements of Jehol Biota (“EEL” assemblage) are clearly recorded in the Hexi Corridor (Zheng et al., 2021), which represents the northwesternmost extent of the Jehol Biota distribution in China, rather than the Junggar Basin (Fig. 1). It seems the Jehol Biota did not migrate to the Junggar Basin in a later stage, probably due to the geographical isolation of the mountain uplifts between the Junggar Basin and Hexi Corridor, including the easternmost Tianshan and Beishan. Low-temperature thermochronology studies indicate Early Cretaceous (ca. 130–95 Ma) exhumation in Beishan (Gillespie et al., 2017a), and Late Cretaceous (ca. 80 Ma) exhumation in the easternmost Tianshan (Gillespie et al., 2017b). The uplift age of Beishan covers the age of the late Jehol Biota, which probably prevented the Jehol Biota from reaching the Junggar Basin during the Early Cretaceous.

- the Ordos Basin, Inner Mongolia: *Canadian Journal of Earth Sciences*, v. 30, p. 2128–2138, <https://doi.org/10.1139/e93-184>.
- Brinkman, D.B., Eberth, D.A., Ryan, M.J., and Chen, P., 2001, The occurrence of *Psittacosaurus xinjiangensis* Sereno and Chow, 1988 in the Urho area, Junggar Basin, Xinjiang, People's Republic of China: *Canadian Journal of Earth Sciences*, v. 38, p. 1781–1786, <https://doi.org/10.1139/e01-049>.
- Brown, B., 1933, An ancestral crocodile: *American Museum Novitates*, v. 638, p. 1–4.
- Brusatte, S.L., Benson, R.B.J., Chure, D.J., Xu, X., Sullivan, C., and Hone, D.E.W., 2009, The first definitive carcharodontosaurid (Dinosauria: Theropoda) from Asia and the delayed ascent of tyrannosaurids: *Naturwissenschaften*, v. 96, p. 1051–1058, <https://doi.org/10.1007/s00114-009-0565-2>.
- Buffetaut, E., 1996, The “ornithurine” bird from the Lower Cretaceous of Changji, Xinjiang (China): Bird or pterosaur?: *Cretaceous Research*, v. 17, p. 505–508, <https://doi.org/10.1006/cretres.1996.0030>.
- Chang, S.-C., Zhang, H., Renne, P.R., and Fang, Y., 2009, High-precision $^{40}\text{Ar}/^{39}\text{Ar}$ age for the Jehol Biota: *Palaeogeography, Palaeoclimatology, Palaeoecology*, v. 280, p. 94–104, <https://doi.org/10.1016/j.palaeo.2009.06.021>.
- Chen, H., Jiang, S., Kellner, A.W.A., Cheng, X., Zhang, X., Qiu, R., Li, Y., and Wang, X., 2020, New anatomical information on *Dsungaripterus weii* Young, 1964 with focus on the palatal region: *PeerJ*, v. 8, <https://doi.org/10.7717/peerj.8741>.
- Chen, P., 1994, Cretaceous conchostracan faunas of China: *Cretaceous Research*, v. 15, p. 259–269, <https://doi.org/10.1006/cretres.1994.1016>.
- Chen, P., 1999, Distribution and spread of the Jehol Biota: *Palaeoworld*, v. 11, p. 1–6.
- Chen, P., 2003, Jurassic biostratigraphy of China, in Zhang, W., Chen, P., and Palmer, A.R., eds., *Biostratigraphy of China*: Beijing, Science Press, p. 423–463.
- Chen, P., and Wei, J., 1985, Lower Cretaceous conchostracans from the Tugulu Group of Xinjiang, in *Collected Works Researching on Geology of Xinjiang*, Institute of Geological Sciences, Xinjiang Geological Bureau: Ürümqi, Xinjiang, China, Xinjiang People Publishing House, p. 131–138.
- Conrad, J.L., and Daza, J.D., 2015, Naming and diagnosing the Cretaceous gekkonomorph (Reptilia, Squamata) from Öösh (Övörkhangai, Mongolia): *Journal of Vertebrate Paleontology*, v. 35, <https://doi.org/10.1080/02724634.2015.980891>.
- Cuenca-Bescós, G., and Canudo, J.L., 2003, A new gobiconodontid mammal from the Early Cretaceous of Spain and its palaeogeographic implications: *Acta Palaeontologica Polonica*, v. 48, p. 575–582.
- Danilov, I.G., and Parham, J.F., 2007, The type series of “*Sinemys wuerhoensis*, a problematic turtle from the Lower Cretaceous of China, includes at least three taxa: *Palaeontology*, v. 50, p. 431–444, <https://doi.org/10.1111/j.1475-4983.2006.00632.x>.
- Dong, Z., 1973, Dinosaurs from Wuerho: *Memoirs of the Institute of Vertebrate Paleontology and Paleoanthropology: Academia Sinica*, v. 11, p. 45–52.
- Dong, Z., 1993, A new species of stegosaur (Dinosauria) from the Ordos Basin, Inner Mongolia, People's Republic of China: *Canadian Journal of Earth Sciences*, v. 30, p. 2174–2176, <https://doi.org/10.1139/e93-188>.
- Eberth, D.A., Brinkman, D.B., Chen, P., Yuan, F., Wu, S., Li, G., and Cheng, X., 2001, Sequence stratigraphy, paleoclimate patterns, and vertebrate fossil preservations in Jurassic–Cretaceous strata of the Junggar Basin, Xinjiang Autonomous Region, People's Republic of China: *Canadian Journal of Earth Sciences*, v. 38, p. 1627–1644, <https://doi.org/10.1139/e01-067>.
- Fang, Y., Olsen, P., Zheng, D., Xue, N., Wang, H., Xu, C., Li, S., Wang, B., and Zhang, H., 2022, A new astronomical time scale for the early Jehol Biota in the Luoping Basin, northeastern China: *Palaeogeography, Palaeoclimatology, Palaeoecology*, v. 607, <https://doi.org/10.1016/j.palaeo.2022.111273>.
- Gillespie, J., Glorie, S., Xiao, W., Zhang, Z., Collins, A.S., Evans, N., McInnes, B., and De Grave, J., 2017a, Mesozoic reactivation of the Beishan, southern Central Asian orogenic belt: Insights from low-temperature thermochronology: *Gondwana Research*, v. 43, p. 107–122, <https://doi.org/10.1016/j.gr.2015.10.004>.
- Gillespie, J., Glorie, S., Jepsen, G., Zhang, Z., Xiao, W., Danišik, M., and Collins, A.S., 2017b, Differential exhumation and crustal tilting in the easternmost Tianshan (Xinjiang, China), revealed by low-temperature thermochronology: *Tectonics*, v. 36, p. 2142–2158, <https://doi.org/10.1002/2017TC004574>.
- He, H., Wang, X., Jin, F., Zhou, Z., Wang, F., Ding, X., Boven, A., and Zhu, R., 2006, $^{40}\text{Ar}/^{39}\text{Ar}$ dating of the early Jehol Biota from Fengning, Hebei Province, northern China: *Geochemistry, Geophysics, Geosystems*, v. 7, no. 4, <https://doi.org/10.1029/2005GC001083>.
- Hone, D.W.E., Jiang, S., and Xu, X., 2018, A taxonomic revision of *Noripterus complicidens* and Asian members of the *Dsungaripteridae*, in Hone, D.W.E., Witton, M.P., and Martill, D.M., eds., *New Perspectives on Pterosaur Palaeobiology*: Geological Society, London, Special Publication 455, p. 149–157, <https://doi.org/10.1144/SP455.8>.
- Ji, L., 1994, The provincialization position and the paleoclimate of the Early Cretaceous microflora in the Minhe Basin, Gansu Province: *Acta Sedimentologica Sinica (Chenji Xuebao)*, v. 12, p. 133–142 [in Chinese].
- Jiang, B., Sha, J., and Cai, H., 2007, Early Cretaceous non-marine bivalve assemblages from the Jehol Group in western Liaoning, northeast China: *Cretaceous Research*, v. 28, p. 199–214, <https://doi.org/10.1016/j.cretres.2006.05.013>.
- Kobayashi, Y., and Lü, J., 2003, A new ornithomimid dinosaurian with gregarious habits from the Late Cretaceous of China: *Acta Palaeontologica Polonica*, v. 48, p. 235–259.
- Ksepka, D.T., Gao, K., and Norell, M., 2005, A new Choristodere from the Cretaceous of Mongolia: *American Museum Novitates*, v. 3468, p. 1–22, [https://doi.org/10.1206/0003-0082\(2005\)468<0001:ANCFTC>2.0.CO;2](https://doi.org/10.1206/0003-0082(2005)468<0001:ANCFTC>2.0.CO;2).
- Li, D., and Ji, S., 2010, New material of the Early Cretaceous pterosaur *Dsungaripterus weii* from northern Xinjiang, Northwest China: *Acta Geoscientia Sinica (Diqui Xuebao)*, v. 31, p. 38–39 [in Chinese].
- Li, D., Zhou, C., Li, L., Yang, J., Li, L., and Rabi, M., 2019, The sinemydid turtle *Ordosemys* from the Lower Cretaceous Mengyin Formation of Shandong, China, and its implication for the age of the Luohandong Formation of the Ordos Basin: *PeerJ*, v. 7, <https://doi.org/10.7717/peerj.6229>.
- Li, G., Shen, Y., and Batten, D.J., 2007, *Yanjiestheria*, *Yanshania* and the development of the *Eosestheria* conchostracan fauna of the Jehol Biota in China: *Cretaceous Research*, v. 28, p. 225–234, <https://doi.org/10.1016/j.cretres.2006.07.002>.
- Li, J., 1985, A revision of *Edentosuchus tienshanensis* Young from the Tugulu Group of Xinjiang Autonomous Region: *Vertebrata Palasiatica*, v. 23, p. 196–206.
- Li, Y., Jiang, S., and Wang, X., 2020, The largest species of *Acanopodus* footprints from Junggar Basin, Xinjiang, China: *Chinese Science Bulletin*, v. 65, p. 1875–1887 [in Chinese], <https://doi.org/10.1360/TB-2019-0513>.
- Li, Y., Jicha, B.R., Yu, Z., Wu, H., Wang, X., Singer, B.S., He, H., and Zhou, Z., 2022, Rapid preservation of Jehol Biota in Northeast China from high precision $^{40}\text{Ar}/^{39}\text{Ar}$ geochronology: *Earth and Planetary Science Letters*, v. 594, <https://doi.org/10.1016/j.epsl.2022.117718>.
- Lü, J., Azuma, Y., Dong, Z., Barsbold, R., Kobayashi, Y., and Lee, Y.N., 2009, New material of *Dsungaripterid* pterosaurs (Pterosauria: Pterodactyloidea) from western Mongolia and its palaeoecological implications: *Geological Magazine*, v. 146, p. 690–700, <https://doi.org/10.1017/S0016756809006414>.
- Lucas, S.G., 2006, The *Psittacosaurus* biochron: Early Cretaceous of Asia: *Cretaceous Research*, v. 27, p. 189–198, <https://doi.org/10.1016/j.cretres.2005.11.011>.
- Lukashевич, E.D., and Przhiborov, A.A., 2015, A new tribe of Diamesinae (Diptera: Chironomidae) from the Lower Cretaceous of Mongolia: *Cretaceous Research*, v. 52, p. 562–569, <https://doi.org/10.1016/j.cretres.2014.03.016>.
- Maisch, M., Matzke, A., and Sun, G., 2003, A new sinemydid turtle (Reptilia: Testudines) from the Lower Cretaceous of the Junggar Basin (NW China): *Neues Jahrbuch für Geologie und Paläontologie, Monatshefte*, v. 12, p. 705–722, <https://doi.org/10.1127/njgpm/2003/2003/705>.
- Maisch, M.W., Matzke, A.T., and Sun, G., 2004, A new dsungaripteroid pterosaur from the Lower Cretaceous of the southern Junggar Basin, north-west China: *Cretaceous Research*, v. 25, p. 625–634, <https://doi.org/10.1016/j.cretres.2004.06.002>.
- Martill, D.M., Frey, E., Chong, D.G., and Bell, C.M., 2000, Reinterpretation of a Chilean pterosaur and the occurrence of *Dsungaripteridae* in South America: *Geological Magazine*, v. 137, p. 19–25, <https://doi.org/10.1017/S0016756800003502>.
- Matzke, A.T., and Maisch, M.W., 2004, New information and specimens of *Wuguia hutubeiensis* (Reptilia: Testudines) from the Lower Cretaceous Tugulu Group of the southern Junggar Basin (NW China): *Neues Jahrbuch für Geologie und Paläontologie, Monatshefte*, v. 8, p. 473–495, <https://doi.org/10.1127/njgpm/2004/2004/473>.
- Osborn, H.F., 1924, Sauropoda and Theropoda from the Lower Cretaceous of Mongolia: *American Museum Novitates*, v. 128, p. 1–7.
- Pan, H., Xu, L., Pan, Z., and Jia, S., 2014, Early Cretaceous non-marine Gastropoda from the dinosaur-bearing strata in Ruyang Basin, Henan Province: *Acta Palaeontologica Sinica*, v. 53, p. 315–326, <https://doi.org/10.19800/j.cnki.aps.2014.03.006>.
- Pol, D., Ji, S., Clark, J.M., and Chiappe, L.M., 2004, Basal crocodyliforms from the Lower Cretaceous Tugulu Group (Xinjiang, China), and the phylogenetic position of *Edentosuchus*: *Cretaceous Research*, v. 25, p. 603–622, <https://doi.org/10.1016/j.cretres.2004.05.002>.
- Rabi, M., Joyce, W.G., and Wings, O., 2010, A review of the Mesozoic turtles of the Junggar Basin (Xinjiang, north-west China) and the paleobiogeography of Jurassic to Early Cretaceous Asian testudines: *Palaeobiodiversity and Palaeoenvironments*, v. 90, p. 259–273, <https://doi.org/10.1007/s12549-010-0031-3>.
- Rauhut, O.W.M., and Xu, X., 2005, The small theropod dinosaurs *Tigulosa* and *Phaedrolosaurus* from the Early Cretaceous of Xinjiang, China: *Journal of Vertebrate Paleontology*, v. 25, p. 107–118, [https://doi.org/10.1671/0272-4634\(2005\)025\[0107:TSTDTA\]2.0.CO;2](https://doi.org/10.1671/0272-4634(2005)025[0107:TSTDTA]2.0.CO;2).
- Sereno, P.C., and Chao, S.C., 1988, *Psittacosaurus xinjiangensis* (Ornithischia: Ceratopsia), a new psittacosaur from the Lower Cretaceous of northwestern China: *Journal of Vertebrate Paleontology*, v. 8, p. 353–365, <https://doi.org/10.1080/02724634.1988.10011724>.
- Su, D., 1980, On late Mesozoic fish fauna from Sinjiang, China: *Vertebrata Palasiatica*, v. 18, p. 76–80.
- Sukhanov, V.B., 2000, Mesozoic turtles of Middle and Central Asia, in Benton, M.J., Shishkin, M.A., Unwin, D.M., and Kurochkin, E.N., eds., *The Age of Dinosaurs in Russia and Mongolia*: Cambridge University Press, p. 309–367.
- Tong, H., Ji, S., and Ji, Q., 2004, *Ordosemys* (Testudines: Cryptodira) from the Yixian Formation of Liaoning Province, northeastern China: New specimens and systematic revision: *American Museum Novitates*, v. 3438, p. 1–20, [https://doi.org/10.1206/0003-0082\(2004\)438<0001:OTCFTY>2.0.CO;2](https://doi.org/10.1206/0003-0082(2004)438<0001:OTCFTY>2.0.CO;2).
- Wang, J., Ye, Y., Pei, R., Tian, Y., Feng, C., Zheng, D., and Chang, S.-C., 2018, Age of Jurassic basal sauropods in Sichuan, China: A reappraisal of basal sauropod evolution: *Geological Society of America Bulletin*, v. 130, no. 9–10, p. 1493–1500, <https://doi.org/10.1130/B31910.1>.
- Wang, S., 2013, The Late Jurassic–early Early Cretaceous new clam shrimp fossils from north China: *Geological Bulletin of China*, v. 32, p. 957–966 [in Chinese].
- Wang, S., Pang, Q., and Wang, D., 2012, New advances in the study of Jurassic–Cretaceous biostratigraphy and isotopic ages of the Junggar Basin in Xinjiang and their significance: *Geological Bulletin of China*, v. 31, p. 493–502 [in Chinese].
- Wang, X., Kellner, A.W.A., Jiang, S., Wang, Q., Ma, Y., Paidoula, Y., Cheng, X., Rodrigues, T., Meng, X., Zhang, J., Li, N., and Zhou, Z., 2014, Sexually dimorphic tridimensionally preserved pterosaurs and their eggs from China: *Current Biology*, v. 24, p. 1323–1330, <https://doi.org/10.1016/j.cub.2014.04.054>.

- Wang, X., Kellner, A.W.A., Jiang, S., Cheng, X., Wang, Q., Ma, Y., Paidoula, Y., Rodrigues, T., Chen, H., Sayão, J.M., Li, N., Zhang, J., Bantim, R.A.M., Meng, X., Zhang, X., Qiu, R., and Zhou, Z., 2017, Egg accumulation with 3D embryos provides insight into the life history of a pterosaur: *Science*, v. 358, no. 6367, p. 1197–1201, <https://doi.org/10.1126/science.aan2329>.
- Wei, J., 1982, Fossil assemblage sequences of Late Permian, Mesozoic and Cenozoic bivalves in Xinjiang and their significance for stratigraphic division, correlation and palaeoclimate: *Xinjiang Petroleum Geology*, v. 1, p. 1–58 [in Chinese].
- Wings, O., Schwarz-Wings, D., Pfretzschner, H.U., and Martin, T., 2010, Overview of Mesozoic crocodylomorphs from the Junggar Basin, Xinjiang, northwest China, and description of isolated crocodyliform teeth from the Late Jurassic Liuhuangou locality: *Palaeobiodiversity and Palaeoenvironments*, v. 90, p. 283–294, <https://doi.org/10.1007/s12549-010-0033-1>.
- Xing, L., Avanzini, M., Lockley, M.G., Miyashita, T., Klein, H., Zhang, J., He, Q., Qi, L., Divay, J.D., and Jia, C., 2014, Early Cretaceous turtle tracks and skeletons from the Junggar Basin, Xinjiang, China: *Palaos*, v. 29, p. 137–144, <https://doi.org/10.2110/palo.2014.012>.
- Xu, X., Zhou, Z., Wang, Y., and Wang, M., 2020, Study on the Jehol Biota: Recent advances and future prospects: *Science China: Earth Sciences*, v. 63, p. 757–773, <https://doi.org/10.1007/s11430-019-9509-3>.
- Yeh, X.-K., 1973, Chelonia fossils from Wuerho: *Memoir of the Institute of Vertebrate Palaeontology and Paleoanthropology: Academia Sinica*, v. 11, p. 8–12 [in Chinese].
- Young, C.-C., 1944, On the reptilian remains from Weiyuan, Szechuan, China: *Bulletin of the Geological Society of China*, v. 24, p. 187–209, <https://doi.org/10.1111/j.1755-6724.1944.mp243-4005.x>.
- Young, C.-C., 1964, On a new pterosaurian from Sinkiang: *Vertebrate Palaeontologia*, v. 8, p. 221–225 [in Chinese].
- Young, C.-C., 1973, Pterosaurian fauna from Wuerho, Sinkiang: *Memoir of the Institute of Vertebrate Palaeontology and Paleoanthropology: Academia Sinica*, v. 11, p. 18–35 [in Chinese].
- Yu, J., Sun, M., Zhang, W., Qu, L., Hou, J., Yang, J., and Sun, S., 1986, Palynological assemblage sequence from the Late Permian to Tertiary in northern Xinjiang: *Bulletin of the Institute of Geology: Chinese Academy of Geosciences*, v. 15, p. 149–163 [in Chinese].
- Yu, Z., Qin, Z., Xi, D., Deng, C., He, H., and Zhou, Z., 2022, New geochronology of the Lower Cretaceous in the Luanping Basin, northern Hebei: Age constraints on the development of early Jehol Biota: *Palaeogeography, Palaeoclimatology, Palaeoecology*, v. 586, <https://doi.org/10.1016/j.palaeo.2021.110768>.
- Zhang, L., Zheng, D., Chang, S.C., Fang, Y., Li, Y., Wang, B., and Zhang, H., 2022, New age constraints on the early Jehol Biota of Luanping, northeastern China: *Palaeogeography, Palaeoclimatology, Palaeoecology*, v. 585, <https://doi.org/10.1016/j.palaeo.2021.110748>.
- Zhang, M., Ji, L., Du, B., Dai, S., and Hou, X., 2015, Palynology of the Early Cretaceous Hanxia section in the Jiuguan Basin, northwest China: The discovery of diverse early angiosperm pollen and paleoclimatic significance: *Palaeogeography, Palaeoclimatology, Palaeoecology*, v. 440, p. 297–306, <https://doi.org/10.1016/j.palaeo.2015.09.010>.
- Zhao, X., 1980, *The Mesozoic Vertebrate Fossils and Stratigraphy in Northern Xinjiang*: Beijing, Science Press, 120 p.
- Zheng, D., Wang, H., Li, S., Wang, B., Jarzembowski, E.A., Dong, C., Fang, Y., Teng, X., Yu, T., Yang, L., Li, Y., Zhao, X., Xue, N., Chang, S.-C., and Zhang, H., 2021, Synthesis of a chrono- and biostratigraphical framework for the Lower Cretaceous of Jiuguan, NW China: Implications for major evolutionary events: *Earth-Science Reviews*, v. 213, <https://doi.org/10.1016/j.earscirev.2020.103474>.
- Zhong, Y., Huyskens, M.H., Yin, Q., Wang, Y., Ma, Q., and Xu, Y., 2021, High-precision geochronological constraints on the duration of ‘Dinosaur Pompeii’ and the Yixian Formation: *National Science Review*, v. 8, <https://doi.org/10.1093/nsr/nwab063>.
- Zhou, C., Wu, W., and Rabi, M., 2019, Presence of the Jehol Biota turtle *Ordosemys liaoxiensis* in the Early Cretaceous Hengtongshan Formation of southern Jilin Province, China: *Fossil Record (Weinheim)*, v. 22, p. 57–64, <https://doi.org/10.5194/fr-22-57-2019>.
- Zhou, Z., Barrett, P.M., and Hilton, J., 2003, An exceptionally preserved Lower Cretaceous ecosystem: *Nature*, v. 421, p. 807–814, <https://doi.org/10.1038/nature01420>.
- Zhou, Z., Meng, Q., Zhu, R., and Wang, M., 2021, Spatiotemporal evolution of the Jehol Biota: Responses to the North China craton destruction in the Early Cretaceous: *Proceedings of the National Academy of Sciences of the United States of America*, v. 118, <https://doi.org/10.1073/pnas.2107859118>.

SCIENCE EDITOR: MIHAI DUCEA
ASSOCIATE EDITOR: PENGFEI LI

MANUSCRIPT RECEIVED 11 OCTOBER 2022
REVISED MANUSCRIPT RECEIVED 10 FEBRUARY 2023
MANUSCRIPT ACCEPTED 24 FEBRUARY 2023

Printed in the USA

1 Zheng, D., Chang, S.-C., Ramezani, J., Xu, X., Xu, H., Wang, H., Pei, R., Fang, Y.,
2 Wang, J., Wang, B., and Zhang, H., 2023, Calibrating Early Cretaceous Urho Pterosaur
3 Fauna in the Junggar Basin and implications for the evolution of the Jehol Biota: GSA
4 Bulletin, <https://doi.org/10.1130/B36795.1>.

6 Supplemental Material

7
8 **Supplemental Text S1.** Stratigraphic information, U-Pb geochronology by LA-MC-ICP-
9 MS, and U-Pb geochronology by CA-ID-TIMS.

10 **Figure S1.** Cathodoluminescent images of zircons from sample W-1 with youngest ages
11 analyzed by LA-MC-ICP-MS U-Pb dating.

12 **Figure S2.** Rank order plot of LA-MC-ICP-MS U-Pb ages for youngest zircon
13 subpopulations from sample W-1.

14 **Table S1.** Vertebrate and trace fossils from the Tugulu Group of the Junggar Basin.

15 **Table S2.** LA-MC-ICP-MS U-Pb analytical results for standard zircons and sample W-1.

16 **Table S3.** CA-ID-TIMS U-Pb analytical results for sample W-1.

17

18

19

20

21

22

23

24

25

26

27

28

29

30

31

32 **Supplemental Text S1**

33 **Stratigraphic information**

34 Abundant fossils, especially belonging to vertebrates, have been reported from the
35 Tugulu Group (Table S1). These include diverse pterosaur, plesiosaur, dinosaur,
36 crocodylomorph, fish, turtle, conchostracan, bivalve, ostracod, charophyte, and
37 sporopollen fossils. In the southern Junggar Basin, the Tugulu Group consists of the
38 Qingshuihe, Hutubihe, Shengjinkou, and Lianmuqin formations. The Qingshuihe
39 Formation is absent in the NW Junggar Basin (Zhao, 1980).

40 In Urho, the Hutubihe Formation unconformably overlies a thick Devonian
41 conglomerate, reaches 150 m thickness, and consists primarily of grey-green, grey-
42 yellow conglomerate, sandstone, and red-brown, grey-green mudstone. Mudstone in the
43 lower Hutubihe Formation hosts vertebrate fossils including material from pterosaurs,
44 plesiosaurs, crocodylomorphs, and dinosaurs. These fossils however have not been
45 systematically interpreted (Zhao, 1980). Hundreds of bird, theropod, stegosaur,
46 pterosaur, and turtle tracks also occur in upper layers of this formation.

47 The Shengjinkou Formation conformably overlies the Hutubihe Formation and
48 conformably underlies the Lianmuqin Formation. It consists of a series of thick, grey-
49 green, grey-yellow sandstones interbedded with mudstone and reaching a cumulative
50 thickness of ca. 250 m. The lowermost Shengjinkou Formation includes a yellow
51 conglomerate that grades into an uppermost white tuffaceous siltstone (0.2 m thick).
52 Vertebrate fossils occur in the grey-green mudstone. These belong to the pterosaurs
53 *Dsungaripterus weii* and *Noriopterus complicidens* and the dinosaur Camarasauridae
54 indet. (Young, 1973; Zhao, 1980; Wings et al., 2010).

55 The Lianmuqin Formation unconformably underlies the Upper Cretaceous Ailike
56 Formation. The Lianmuqin Formation consists primarily of grey-green sandstone, grey-
57 yellow sandy mudstone, and red-brown mudstone reaching a cumulative thickness of ca.
58 430 m. Vertebrate fossils in the sandstone and mudstone include the pterosaurs
59 *Dsungaripterus weii*, *Noriopterus complicidens*, the plesiosaur *Sinopliosaurus*
60 *weiyuanensis*, turtles *Xinjiangchelys* sp., *Ordosemys brinkmania*, and cf. *Pantrionychia*,
61 the crocodylomorph *Edentosuchus tienshanensis*, and the dinosaurs *Tugulusaurus faciles*,
62 *Phaedrolosaurus ilikensis*, *Xinjiangovenator parvus*, *Kelmaysaurus petrolicus*, cf.
63 *Asiatosaurus mongoliensis*, *Psittacosaurus xinjiangensis*, and *Wuerhosaurus homheni*
64 (Young, 1964, 1973; Dong, 1973; Li, 1985; Brinkman et al., 2001; Pol et al., 2004;
65 Rauhut and Xu, 2005; Danilov and Parham, 2007; Wings et al., 2010).

66 At the Jiamuhe section an isolated, white, tuffaceous horizon occurs at the
67 boundary between the Shengjinkou and Lianmuqin formations (Figs. 2C, 3 and 5). The
68 tuffaceous marker bed is approximately 20 cm thick, is laterally continuous in the outcrop
69 and exhibits sharp contacts with the enclosing sandstones and siltstones. It locally
70 diverges into separate, closely spaced tuffaceous layers interbedded with the latter
71 lithologies (Fig. 3). The tuffaceous siltstone is soft, clay-rich and friable when dry.

72

73 **U-Pb geochronology by LA-MC-ICP-MS**

74 The tuffaceous sample W-1 from the Jiamuhe section was mechanically crushed
75 and underwent mineral separation using standard sieving, magnetic, and high-density
76 liquid techniques. Zircons were then manually selected using a binocular microscope.
77 One hundred small, inclusion-free, zircon grains (40–70 μm in length) from the sample

78 were mounted in epoxy resin. Hardened mounts were polished to expose zircon grain
79 midsections to about one-half of their width. Cathodoluminescence (CL) imaging was
80 used to document grain morphologies and internal structure for *in situ* analysis (fig. S2).
81 U-Pb isotopic data on zircons were measured at the Department of Earth Sciences,
82 University of Hong Kong, using a Nu Instruments Multi-Collector (MC) ICP-MS with a
83 Resonetics RESolution M-50-HR Excimer Laser Ablation System. The analyses used a
84 beam diameter of 30 μm , repetition rate of 4 Hz, and energy density of 5 J/cm^2 on the
85 sample surface. The average ablation time was approximately 25 s, and pit depths
86 reached about 20 to 30 μm . The standard zircons 91500 (Wiedenbeck, 1995) and GJ-1
87 (Jackson et al., 2004) were used for data validation. The zircon 91500 was used as an
88 external calibration standard to evaluate the magnitude of mass bias and inter-elemental
89 fractionation. The zircon GJ-1 was used to evaluate the accuracy and reproducibility of
90 the laser ablation results. The software ICPMSDataCal Version 8.0 (Liu et al., 2010) was
91 used to process the off-line signal selection, quantitative calibration, and time-drift
92 correction. We used a function given in Anderson (Anderson, 2002) to correct for
93 common Pb in Microsoft Excel. Concordant and rank order plots were created using
94 ISOPLOT/Excel version 3.0 (Ludwig, 2003).

95 In this study, 20 zircon grains were randomly selected from the sample so that the
96 results would capture the overall character of the age populations. $^{206}\text{Pb}/^{238}\text{U}$ ages were
97 interpreted for zircon grains younger than 1000 Ma, and $^{207}\text{Pb}/^{206}\text{Pb}$ ages were interpreted
98 for older grains. Ages were retained only for analyses exhibiting concordance of 95% or
99 more and after excluding distinguishably older (detrital) analyses. Table S1 lists U-Pb
100 data results. Average 2σ analytical uncertainty was ± 1.6 myr for the analyzed zircons of

101 Cretaceous age. The sample age is derived from the weighted mean $^{206}\text{Pb}/^{238}\text{U}$ date of
102 nine youngest analyses with its 95% confidence level uncertainty reported using $\pm \alpha/\beta$
103 Ma notation, where α is the internal (analytical) uncertainty in the absence of all external
104 errors, and β incorporates α as well as the external reproducibility (age bias). β must be
105 taken into account when comparing U-Pb ages measured by different analytical
106 techniques (e.g., *in situ* dating versus ID-TIMS). Analysis of the 6 secondary standard
107 GJ-1 in the present study provides an age of 601.6 ± 1.9 Ma. Considering that the
108 accepted age for GJ-1 (Hortswood et al. 2016) is 601.95 ± 0.40 Ma, our analyses are off
109 target by 0.25%. 0.25% of 135.2 Ma is 0.34 m.y. Then we can calculate the β error:
110 $\text{SQRT}((0.5^2) + (0.34^2)) = 0.6$ m.y.

111

112 **U-Pb geochronology by CA-ID-TIMS**

113 A set of zircons from sample W-1 were analyzed by the high-precision CA-ID-
114 TIMS method following the procedures described in Ramezani et al. (2022). Zircons
115 were pre-treated using a chemical abrasion technique modified after Mattinson (2005).
116 This involved thermal annealing in a furnace at 900°C for 60 hours, followed by partial
117 dissolution in 29 M HF at 210°C in high-pressure vessels for 12 hours. This procedure
118 mitigates the effects of radiation-induced Pb loss in zircon and thus improves the
119 accuracy of U-Pb dates. (Removal of Pb-loss areas is not possible with *in situ* dating
120 techniques.) The chemically abraded grains were successively fluxed in several hundred
121 microliters of dilute HNO_3 and 6M HCl on a hot plate and in an ultrasonic bath (1 hour
122 each). Material was rinsed with several volumes of Millipore water in between fluxes to
123 remove the leachates.

124 Pretreated zircon grains were spiked with a mixed ^{205}Pb - ^{233}U - ^{235}U isotopic tracer
125 (ET535; Condon et al., 2015; McLean et al., 2015) prior to complete dissolution in 29 M
126 HF at 210°C for 48 hours and subsequent Pb and U purification via an HCl-based anion-
127 exchange column chemistry (Krogh, 1973). Purified Pb and U were loaded together onto
128 single outgassed Re filaments along with a silica-gel emitter solution. Their isotopic
129 ratios were measured using an Isotopx X62 multi-collector thermal ionization mass
130 spectrometer equipped with a Daly photomultiplier ion-counting system at the
131 Massachusetts Institute of Technology Isotope Laboratory. Pb isotopes were measured as
132 mono-atomic ions in peak-hopping mode on the ion-counter and were corrected for a
133 mass-dependent isotope fractionation of $0.18\% \pm 0.05\%$ per atomic mass unit (2σ). U
134 isotopes were measured as dioxide ions in static mode using three Faraday collectors.
135 Ratios were subjected to an oxide correction using an independently determined $^{18}\text{O}/^{16}\text{O}$
136 ratio of 0.00205 ± 0.00005 . Within-run U mass fractionation corrections were made using
137 the $^{233}\text{U}/^{235}\text{U}$ ratio of the tracer and a predicted sample $^{238}\text{U}/^{235}\text{U}$ ratio of 137.818 ± 0.045
138 (Hiess et al., 2012).

139 A total of 5 zircons from sample W-1 were analysed by the CA-ID-TIMS method.
140 Table S2 lists complete Pb and U isotopic data and Figure 3b shows age results as ranked
141 age plots. Data reduction, calculation of dates, and propagation of uncertainties used the
142 Tripoli and ET_Redux applications and algorithms (Bowring et al., 2011; McLean et al.,
143 2011). The individual $^{206}\text{Pb}/^{238}\text{U}$ dates were corrected for initial ^{230}Th disequilibrium
144 based on an assumed magma Th/U ratio of 2.8 ± 1.0 (2σ). The 2σ analytical uncertainty
145 of individual zircon dates ranged from ± 0.34 myr to ± 0.92 myr. The relatively high

146 uncertainty of the CA-ID-TIMS method here is due to the small zircon size and thus
147 small amounts of measured radiogenic Pb (<2.5 pg) and U (<100 pg).

148

149 **References cited**

150 Augustin, F.J., Matzke, A.T., Maisch, M.W., and Pfretzschner, H.-U., 2021, New
151 information on *Lonchognathosaurus* (Pterosauria: Dsungaripteridae) from the
152 Lower Cretaceous of the southern Junggar Basin (NW China): *Cretaceous*
153 *Research*, v. 124, p.104808, <https://doi.org/10.1016/j.cretres.2021.104808>.

154 Augustin, F.J., Matzke, A.T., Maisch, M.W., and Csiki-Sava, Z., 2022a, Pterosaur remains
155 from the Lower Cretaceous Lianmuxin Formation (upper Tugulu Group) of the
156 southern Junggar Basin (NW China): *Historical Biology*, v. 34, p. 312–321, DOI:
157 10.1080/08912963.2021.1910819.

158 Augustin, F.J., Matzke, A.T., Maisch, M.W., Kampouridis, P., and Csiki-Sava, Z., 2022b,
159 The first record of pterosaurs from the Lower Cretaceous Hutubei Formation
160 (lower Tugulu Group) of the southern Junggar Basin (NW China)—A glimpse into
161 an unusual ecosystem: *Cretaceous Research*, v. 130, p. 105066,
162 <https://doi.org/10.1016/j.cretres.2021.105066>.

163 Anderson, T., 2002, Correction of common lead in U–Pb analyses that do not report
164 ²⁰⁴Pb: *Chemical Geology*, v. 192, p. 59–79, [https://doi.org/10.1016/S0009-](https://doi.org/10.1016/S0009-2541(02)00195-X)
165 [2541\(02\)00195-X](https://doi.org/10.1016/S0009-2541(02)00195-X).

166 Bowring, J.F., McLean, N.M., Bowring, S.A., 2011. Engineering cyber infrastructure for
167 U-Pb geochronology: Tripoli and U-Pb_Redux. *Geochem. Geophys. Geosy.* 12,
168 Q0AA19. DOI:10.1029/2010GC003478.

169 Brinkman, D.B., Eberth, D.A., Ryan, M.J., and Chen, P., 2001, The occurrence of
170 *Psittacosaurus xinjiangensis* Sereno and Chow, 1988 in the Urho area, Junggar
171 Basin, Xinjiang, People's Republic of China, in Currie, P., ed., The Sino-Canadian
172 Dinosaur Project 3: Canadian Journal of Earth Sciences, v. 38, p. 1781–1786.

173 Condon, D.J., Schoene, B., McLean, N.M., Bowring, S.A., Parrish, R.R., 2015.
174 Metrology and traceability of U-Pb isotope dilution geochronology
175 (EARTHTIME Tracer Calibration Part I). Geochim. Cosmochim. Ac. 164, 464–
176 480. <https://doi.org/10.1016/j.gca.2015.05.026>.

177 Danilov, I.G., and Parham, J.F., 2007, The type series of '*Sinemys*' *wuerhoensis*, a
178 problematic turtle from the Lower Cretaceous of China, includes at least three
179 taxa: Palaeontology, v. 50, p. 431–444, doi:10.1111/j.1475-4983.2006.00632.x.

180 Dong, Z., 1973, Dinosaurs from Wuerho: Memoirs of the Institute of Vertebrate
181 Paleontology and Paleoanthropology, Academia Sinica, v. 11, p. 45–52.

182 He, Q., Xing, L., Zhang, J., Lockley, M.G., Klein, H., Persons IV, W.S., Qi, L., and Jia,
183 C., 2013, New Early Cretaceous pterosaur–bird track assemblage from Xinjiang,
184 China: palaeoethology and paleoenvironment: Acta Geologica Sinica, v. 87, p.
185 1477–1485, <https://doi.org/10.1111/1755-6724.12151>.

186 Hiess, J., Condon, D.J., McLean, N., Noble, S.R., 2012. $^{238}\text{U}/^{235}\text{U}$ Systematics in
187 Terrestrial Uranium-Bearing Minerals. Science 335, 1610–1614. DOI:
188 10.1126/science.1215507.

189 Hone, D.W.E., Jiang, S., Xu, X., 2018. A taxonomic revision of *Noriopteris complicidens*
190 and Asian members of the Dsungaripteridae. Geol. Soc. Spec. Publ. 455, 149–
191 157. <https://doi.org/10.1144/SP455.8>.

192 Horstwood, M.S.A., et al., 2016. Community-derived standards for LA-ICP-MS U-(Th-
193 Pb geochronology - uncertainty propagation, age Interpretation and data
194 reporting. *Geostand. Geoanal. Res.* 40, 311–332. [https://doi.org/10.1111/j.1751-](https://doi.org/10.1111/j.1751-908X.2016.00379.x)
195 908X.2016.00379.x.

196 Jackson, S.E., Pearson, N.J., Griffin, W.L., and Belousova, E.A., 2004, The application of
197 laser ablation-inductively coupled plasma-mass spectrometry to in situ U–Pb
198 zircon geochronology: *Chemical Geology*, v. 211, p. 47–69,
199 <https://doi.org/10.1016/j.chemgeo.2004.06.017>.

200 Khosatzky, L.I., 1996, New turtle from the Early Cretaceous of Central Asia: *Russian*
201 *Journal of Herpetology*, v. 3, p. 89–94.

202 Krogh, T.E., 1973. Low-Contamination Method for Hydrothermal Decomposition of
203 Zircon and Extraction of U and Pb for Isotopic Age Determinations. *Geochim.*
204 *Cosmochim. Ac.* 37, 485–494. [https://doi.org/10.1016/0016-7037\(73\)90213-5](https://doi.org/10.1016/0016-7037(73)90213-5).

205 Li, D., and Ji, S., 2010, New Material of the Early Cretaceous pterosaur *Dsungaripterus*
206 *Weii* from northern Xinjiang, Northwest China: *Acta Geoscientica Sinica*, v. 31, p.
207 38–39.

208 Li, J., 1985, A revision of *Edentosuchus tienshanensis* Young from the Tugulu Group of
209 Xingjiang Autonomous Region: *Vertebrata Palasiatica*, v. 23, p. 196–206

210 Li, Y., Jiang, S., Wang, X., 2020. The largest species of *Asianopodus* footprints from
211 Junggar Basin, Xinjiang, China (in Chinese). *Chin. Sci. Bull.* 65, 1875–1887.
212 DOI: 10.1360/TB-2019-0513.

213 Liu, Y., Gao, S., Hu, Z., Gao, C., Zong, K., Wang, D., 2010. Continental and oceanic
214 crust recycling-induced melt-peridotite interactions in the trans-north China

215 orogen: U–Pb dating, Hf isotopes and trace elements in zircons from mantle
216 xenoliths. *J. Petrol.* 51, 537–571.

217 Ludwig, K.R., 2003, Isoplot v. 3.0: A geochronological toolkit for Microsoft excel:
218 Special Publication, No. 4. Berkeley Geochronology Center, 70 p.

219 Maisch, M., Matzke, A., and Sun, G., 2003, A new sinemydid turtle (Reptilia: Testudines)
220 from the Lower Cretaceous of the Junggar Basin (NW China): *Neues Jahrbuch für*
221 *Geologie und Paläontologie Monatshefte*, v. 12, p. 705–722.

222 Maisch, M.W., Matzke, A.T., and Sun, G., 2004, A new dsungaripteroid pterosaur from
223 the Lower Cretaceous of the southern Junggar Basin, north-west China:
224 *Cretaceous Research*, v. 25, p. 625–634, doi:10.1007/s12549-010-0031-3.

225 Mattinson, J.M., 2005. Zircon U/Pb chemical abrasion (CA-TIMS) method; combined
226 annealing and multi-step partial dissolution analysis for improved precision and
227 accuracy of zircon ages. *Chem. Geol.* 220, 47–66.
228 <https://doi.org/10.1016/j.chemgeo.2005.03.011>.

229 Matzke, A.T., and Maisch, M.W., 2004, New information and specimens of *Wuguia*
230 *hutubeiensis* (Reptilia: Testudines) from the Lower Cretaceous Tugulu Group of
231 the southern Junggar Basin (NW China): *Neues Jahrbuch für Geologie und*
232 *Paläontologie Monatshefte*, v. 8, p. 473–495.

233 McLean, N.M., Bowring, J.F., Bowring, S.A., 2011. An algorithm for U-Pb isotope
234 dilution data reduction and uncertainty propagation. *Geochem. Geophys. Geosy.*
235 12, Q0AA18. DOI:10.1029/2010GC003479.

236 McLean, N.M., Condon, D.J., Schoene, B., Bowring, S.A., 2015. Evaluating uncertainties
237 in the calibration of isotopic reference materials and multi-element isotopic

238 tracers (EARTHTIME Tracer Calibration Part II). *Geochim. Cosmochim. Ac.* 164,
239 481–501. <https://doi.org/10.1016/j.gca.2015.02.040>.

240 Pol, D., Ji, S., Clark, J.M., and Chiappe, L.M., 2004, Basal crocodyliforms from the
241 Lower Cretaceous Tugulu Group (Xinjiang, China), and the phylogenetic position
242 of *Edentosuchus*: *Cretaceous Research*, v. 25, p. 603–622,
243 <https://doi.org/10.1016/j.cretres.2004.05.002>.

244 Ramezani, J., Beveridge, T. L., Rogers, R. R., Eberth, D. A., and Roberts, E. M., 2022,
245 Calibrating the zenith of dinosaur diversity in the Campanian of the Western
246 Interior Basin by CA-ID-TIMS U–Pb geochronology: *Scientific Reports*, v. 12,
247 no. 1, p. 16026, <https://doi.org/10.1038/s41598-022-19896-w>.

248

249 Rauhut, O.W.M., and Xu, X., 2005, The small theropod dinosaurs *Tugulusaurus* and
250 *Phaedrolosaurus* from the Early Cretaceous of Xinjiang, China: *Journal of*
251 *Vertebrate Paleontology*, v. 25, p. 107–118, [https://doi.org/10.1671/0272-](https://doi.org/10.1671/0272-4634(2005)025[0107:TSTDTA]2.0.CO;2)
252 [4634\(2005\)025\[0107:TSTDTA\]2.0.CO;2](https://doi.org/10.1671/0272-4634(2005)025[0107:TSTDTA]2.0.CO;2).

253 Sereno, P.C., and Chao, S., 1988, *Psittacosaurus xinjiangensis* (Ornithischia: Ceratopsia),
254 a new psittacosaur from the Lower Cretaceous of northwestern China: *Journal of*
255 *Vertebrate Paleontology*, v. 8, p. 353–365,
256 <https://doi.org/10.1080/02724634.1988.10011724>.

257 Su, D., 1980, On late Mesozoic fish fauna from Xinjiang, China: *Vertebrata Palasiatica*,
258 v. 18, p. 76–80.

259 Su, D., 1985, On late Mesozoic fish fauna from Xinjiang (Sinkiang), China: *Memoirs of*
260 *Institute of Vertebrate Palaeontology and Palaeoanthropology, Academia Sinica*, v.

261 17, p. 61–136.

262 Wiedenbeck, M., Alle, P., Corfu, F., Griffin, W.L., Meier, M., Oberli, F., Quadt, A.,
263 Roddick, J.C., and Spiegel, W., 1995, Three natural zircon standards for U–Th–
264 Pb, Lu–Hf, trace element and REE analyses: *Geostandards and Geoanalytical*
265 *Research*, v. 19, p. 1–23, <https://doi.org/10.1111/j.1751-908X.1995.tb00147.x>.

266 Wings, O., Schwarz-Wings, D., Pfretzschner, H.U., and Martin, T., 2010, Overview of
267 Mesozoic crocodylomorphs from the Junggar Basin, Xinjiang, northwest China
268 and description of isolated crocodyliform teeth from the Late Jurassic
269 Liuhuanggou locality, *in* Martin, T., Sun, G., Mosbrugger, V., eds., *Triassic–*
270 *Jurassic Biodiversity, Ecosystems, and Climate in the Junggar Basin, Xinjiang,*
271 *northwest China: Palaeobiodiversity and Palaeoenvironments*, v. 90, p. 283–294,
272 [doi:10.1007/s12549-010-0033-1](https://doi.org/10.1007/s12549-010-0033-1).

273 Xing, L., Avanzini, M., Lockley, M.G., Miyashita, T., Klein, H., Zhang, J., He, Q., Qi,
274 L., Divay, J.D., and Jia, C., 2014, Early Cretaceous turtle tracks and skeletons
275 from the Junggar Basin, Xinjiang, China: *PALAIOS*, v. 29, p. 137–144,
276 <https://doi.org/10.2110/palo.2014.012>.

277 Xing, L., Harris, J.D., Jia, C., Luo, Z., Wang, S., and An, J., 2011, Early Cretaceous bird-
278 dominated and dinosaur footprint assemblages from the northwestern margin of
279 the Junggar Basin, Xinjiang, China: *Palaeoworld*, v. 20, p. 308–321,
280 <https://doi.org/10.1016/j.palwor.2011.01.001>.

281 Xing, L., Lockley, M.G., Klein, H., Zhang, J., He, Q., Divay, J.D., Qi, L., and Jia, C.,
282 2013a, Dinosaur, bird and pterosaur footprints from the Lower Cretaceous of
283 Wuerhe asphaltite area, Xinjiang, China, with notes on overlapping track

284 relationships: Palaeoworld, v. 22, p. 42–51,
285 <https://doi.org/10.1016/j.palwor.2013.03.001>.

286 Xing, L., Lockley, M.G., Mccrea, R.T., Gierliński, G.D., Buckley, L.G., Zhang, J., Qi, L.,
287 and Jia, C., 2013b, First record of *Deltapodus* tracks from the Early Cretaceous of
288 China: Cretaceous Research, v. 42, p. 55–65,
289 <https://doi.org/10.1016/j.cretres.2013.01.006>.

290 Yeh, X.-K., 1973, Chelonia fossils from Wuerho: Memoir of the Institute of Vertebrate
291 Palaeontology and Paleoanthropology, Academia Sinica, v. 11, p. 8–12.

292 Young, C.-C., 1964, On a new pterosaurian from Sinkiang: Vertebrate PalAsiatica, v. 8,
293 p. 221–225.

294 Young, C.-C., 1973, Pterosaurian Fauna from Wuerho, Sinkiang: Memoir of the Institute
295 of Vertebrate Palaeontology and Paleoanthropology, Academia Sinica, v. 11, p.
296 18–35.

297 Zhao, X., 1980, The Mesozoic vertebrate Fossils and Stratigraphy in northern Xinjiang:
298 Science Press, Beijing, 120 p.

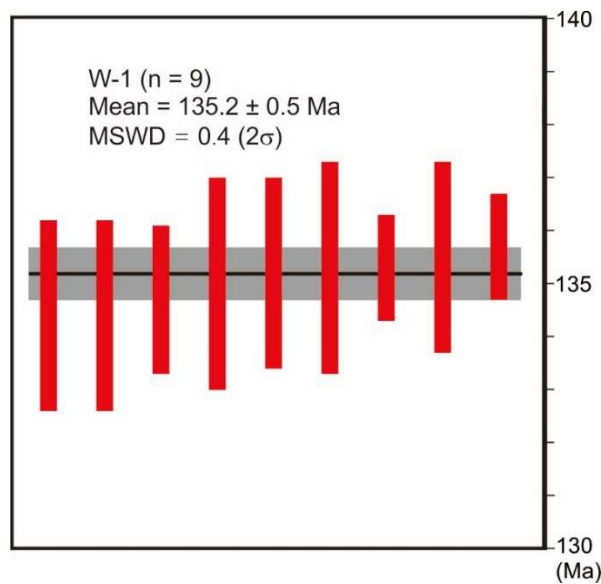
299
300
301
302
303
304
305
306

307 **Figure S1. Cathodoluminescent images of zircons from sample W-1 with youngest**
 308 **ages analyzed by LA-MC-ICP-MS U-Pb dating.** Age uncertainties are given at the 1σ
 309 level.



310
 311

312 **Figure S2. Rank order plot of LA-MC-ICP-MS U-Pb ages for youngest zircon**
 313 **subpopulations from sample W-1.** Horizontal lines in rank order plot signify calculated
 314 sample dates. The width of the shaded band represents internal uncertainty in the
 315 weighted mean age at a 95% confidence level. Age uncertainties are given at the 2σ level.
 316 MSWD—mean square of weighted deviates.



317
 318
 319

320 **Table S1. Vertebrate and trace fossils from the Tugulu Group of the Junggar Basin.**

321 Numbers correspond references: ¹ Young (1964); ² Young (1973); ³ Yeh (1973), Danilov
 322 and Parham (2007); ⁴ Dong (1973); ⁵ Sereno and Chao (1988); ⁶ Young (1973), Li
 323 (1985), Pol et al. (2004), Wings et al. (2004); ⁷ Zhao (1980); ⁸ Xing et al. (2011); ⁹ Xing
 324 et al. (2013a), He et al. (2013); ¹⁰ Xing et al. (2014); ¹¹ Xing et al. (2011), Xing et al.
 325 (2013a); ¹² Xing et al. (2013b); ¹³ Maisch et al. (2004), Augustin et al. (2021); ¹⁴ Augustin
 326 et al. (2022a); ¹⁵ Brinkman (2001); ¹⁶ Maisch et al. (2003), Danilov and Sukhanov
 327 (2006); ¹⁷ Su (1980, 1985); ¹⁸ Augustin et al. (2022b); ¹⁹ Matzke and Maisch (2004); ²⁰
 328 Khosatzky (1996).

		NW Junggar Basin	Southern Junggar Basin
Tugulu Group	Lianmuqin Fm.	pterosaur: <i>Dsungaripterus weii</i> ¹ <i>Noriopteris complicidens</i> ² turtle: <i>Xinjiangchelys</i> sp. ³ <i>Ordosemys brinkmania</i> ³ cf. <i>Pantrionychia</i> indet. ³ dinosaur: <i>Tugulusaurus faciles</i> ⁴ <i>Xinjiangovenator parvus</i> ⁵ <i>Kelmaysaurus petrolicus</i> ⁴ cf. <i>Asiatosaurus mongoliensis</i> ⁴ <i>Psittacosaurus xinjiangensis</i> ⁵ <i>Wuerhosaurus homheni</i> ⁴ plesiosaur <i>Sinopliosaurus weiyuanensis</i> ² crurotarsan: <i>Edentosuchus tienshanensis</i> ⁶	pterosaur: <i>Lonchognathosaurus acutirostris</i> ¹³ Dsungaripteridae indet. ¹⁴ turtle: <i>Dracochelys bicuspis</i> ¹⁵ <i>Wuguia efremovi</i> ¹⁶

	<p>Shengjinkou Fm.</p> <p>pterosaur: <i>Dsungaripterus weii</i>⁷ <i>Noriopterus complicidens</i>⁷</p> <p>dinosaur: Camarasauridae indet.⁷</p>	<p>fish: <i>Uighuroniscus sinkiangensi</i>¹⁷ <i>Manasichthys tuguluensis</i>¹⁷ <i>Dsungarichthys bilineatus</i>¹⁷ <i>Manasichthys elongates</i>¹⁷ <i>Bogdaichthys fukangensis</i>¹⁷ <i>Bogdaichthys serratus</i>¹⁷</p>
	<p>Hutubihe Fm.</p> <p>bird tracks: <i>Koreanaornis dodsoni</i>⁸ <i>Goseongornipes</i> isp.⁸ <i>Aquatilavipes</i> isp.⁸ <i>Moguiornipes robusta</i>⁸</p> <p>pterosaur tracks: <i>Pteraichnus</i> isp.⁹</p> <p>turtle tracks: <i>Chelonipus</i> isp.¹⁰ <i>Emydhopus</i> isp.¹⁰</p> <p>Non-avian theropod tracks: cf. <i>Jialingpus</i> isp.¹¹ <i>Asianopodus</i> isp.⁸ <i>Kayentapus</i> isp.⁸ <i>Deltapodus curriei</i>¹²</p>	<p>pterosaur: Dsungaripteridae indet.¹⁸</p> <p>turtle: <i>Wuguia efremovi</i>¹⁹ <i>Wuguia hutubeiensis</i>²⁰</p>
Qingshuihe Fm.		

Table S2. LA-MC-ICP-MS U-Pb analytical results for standard zircons and sample W-1.

Samples	Isotopic ratios							rho	U-Pb Ages (Ma)						discor.
	Th/U	²⁰⁷ Pb/ ²⁰⁶ Pb	±1σ	²⁰⁷ Pb/ ²³⁵ U	±1σ	²⁰⁶ Pb/ ²³⁸ U	±1σ		²⁰⁷ Pb/ ²⁰⁶ Pb	±1σ	²⁰⁷ Pb/ ²³⁵ U	±1σ	²⁰⁶ Pb/ ²³⁸ U	±1σ	
Standard samples															
91500std	0.345	0.07463	0.00046	1.8446	0.01306	0.1793	0.00083	0.6526	1059	7	1061	5	1063	5	0
91500std	0.345	0.07463	0.00046	1.8446	0.01306	0.1793	0.00083	0.6526	1059	7	1061	5	1063	5	0
91500std	0.35	0.07513	0.00059	1.8558	0.01647	0.1791	0.00079	0.498	1072	11	1065	6	1062	4	0
91500std	0.356	0.07509	0.00043	1.8551	0.0117	0.1791	0.00084	0.7465	1071	6	1065	4	1062	5	0
91500std	0.338	0.07467	0.00044	1.8453	0.01347	0.1792	0.00094	0.7183	1060	7	1062	5	1063	5	0
91500std	0.35	0.07488	0.00048	1.8525	0.014	0.1793	0.00076	0.5638	1065	9	1064	5	1063	4	0
91500std	0.345	0.07488	0.00047	1.848	0.01202	0.179	0.00077	0.6637	1065	7	1063	4	1062	4	0
GJ-1	0.028	0.06023	0.00035	0.8123	0.00548	0.0978	0.00039	0.5857	612	8	604	3	601	2	0
GJ-1	0.028	0.0604	0.00033	0.8151	0.00556	0.0978	0.00042	0.6275	618	8	605	3	602	2	0
GJ-1	0.028	0.05995	0.00029	0.8087	0.00546	0.0978	0.00051	0.7791	602	7	602	3	601	3	0
GJ-1	0.028	0.06022	0.00025	0.8124	0.00476	0.0978	0.00048	0.8314	612	6	604	3	601	3	0
GJ-1	0.027	0.06046	0.00028	0.8169	0.00463	0.098	0.00038	0.6818	620	6	606	3	602	2	1
GJ-1	0.028	0.06042	0.00033	0.8151	0.00475	0.0978	0.00045	0.7884	619	6	605	3	602	3	0
W-01	0.592	0.05651	0.00024	0.6035	0.00569	0.0774	0.00067	0.9238	472	9	479	4	481	4	0
W-02	1.163	0.05238	0.00041	0.373	0.00498	0.0516	0.00052	0.7574	302	14	322	4	324	3	1
W-03	0.704	0.05209	0.0006	0.1519	0.00234	0.0211	0.00011	0.3421	289	25	144	2	134.9	0.7	7
W-04	0.862	0.0652	0.0004	1.1285	0.008	0.1255	0.00053	0.5946	781	8	767	4	762	3	1
W-05	0.68	0.05053	0.00049	0.1479	0.00172	0.0212	0.00015	0.6215	220	14	140	2	135.3	1	3
W-06	0.901	0.05513	0.00528	0.162	0.01548	0.0213	0.00015	0.2749	418	219	152	14	135.9	1	12
W-07	1.266	0.05442	0.00047	0.3317	0.00452	0.0441	0.0003	0.5065	388	18	291	3	278	2	5
W-08	0.99	0.05055	0.00125	0.1472	0.00355	0.0211	0.00011	0.6625	220	58	139	3	134.7	0.7	3
W-09	0.84	0.04914	0.00054	0.1441	0.00176	0.0213	0.00014	0.5547	155	16	137	2	135.5	0.9	1
W-10	0.446	0.04974	0.00149	0.1445	0.0042	0.0211	0.00015	0.4875	183	71	137	4	134.4	0.9	2
W-11	0.595	0.05311	0.00097	0.164	0.00289	0.0224	0.00011	0.6799	333	42	154	3	142.8	0.7	8
W-12	0.415	0.05126	0.00187	0.1489	0.00534	0.0211	0.00015	0.3858	252	86	141	5	134.4	0.9	5
W-13	0.571	0.05184	0.00078	0.1658	0.00223	0.0232	0.00015	0.859	278	35	156	2	147.8	1	6
W-14	1.042	0.05803	0.00073	0.552	0.00612	0.069	0.0004	0.9846	531	28	446	4	430	2	4
W-15	0.337	0.05067	0.0008	0.1482	0.00231	0.0212	0.00009	0.2609	226	28	140	2	135.3	0.5	3

W-16	1.205	0.05023	0.00053	0.1473	0.00151	0.0213	0.00007	0.3375	206	17	140	1	135.7	0.5	3
W-17	0.962	0.05233	0.00044	0.1527	0.00141	0.0212	0.00011	0.5771	300	12	144	1	135	0.7	7
W-18	0.562	0.05363	0.00446	0.1531	0.01266	0.0207	0.00018	0.1703	356	191	145	11	132	1	10
W-19	0.84	0.04924	0.00061	0.144	0.00206	0.0212	0.00015	0.4955	159	20	137	2	135.2	0.9	1
W-20	0.87	0.05046	0.00043	0.1478	0.00179	0.0212	0.00018	0.6822	216	14	140	2	135	1	4

Table S3. CA-ID-TIMS U-Pb analytical results for sample W-1. Zircon number in bold indicates analysis providing maximum depositional age.

Sample Fractions	Pb(c) (pg)	Pb* Pb _c	U (pg)	Th U	Ratios						Ages (Ma)						corr. coef.		
					$\frac{^{206}\text{Pb}}{^{204}\text{Pb}}$	$\frac{^{208}\text{Pb}}{^{206}\text{Pb}}$	$\frac{^{206}\text{Pb}}{^{238}\text{U}}$	err	$\frac{^{207}\text{Pb}}{^{235}\text{U}}$	err	$\frac{^{207}\text{Pb}}{^{206}\text{Pb}}$	err	$\frac{^{206}\text{Pb}}{^{238}\text{U}}$	err	$\frac{^{207}\text{Pb}}{^{235}\text{U}}$	err		$\frac{^{207}\text{Pb}}{^{206}\text{Pb}}$	err
(a)	(b)	(c)	(c)		(d)	(e)	(f)	(2σ%)	(f)	(2σ%)	(f)	(2σ%)	(2σ)		(2σ)		(2σ)		
z3	0.27	3.3	32	1.17	184.9	0.371	0.022194	(.62)	0.15659	(7.40)	0.05119	(7.20)	141.51	0.87	148	10	248	166	0.35
z4	0.47	3.4	71	0.45	224.1	0.143	0.021722	(.48)	0.15231	(5.79)	0.05088	(5.65)	138.53	0.66	143.9	7.8	234	130	0.34
z5	0.45	2.7	51	0.77	170.2	0.243	0.021535	(.64)	0.15509	(7.64)	0.05226	(7.45)	137.35	0.88	146	10	296	170	0.35
z1	0.29	7.9	94	0.90	445.4	0.285	0.021395	(.25)	0.14625	(2.98)	0.04960	(2.90)	136.47	0.34	138.6	3.9	175	68	0.35
z2	0.37	3.1	48	0.83	190.1	0.264	0.021196	(.69)	0.14622	(8.24)	0.05006	(7.95)	135.21	0.92	139	11	197	185	0.47

Notes:

(a) Thermally annealed and pre-treated single zircon.

(b) Total common-Pb in analyses.

(c) Total sample U content.

(d) Measured ratio corrected for spike and fractionation only.

(e) Radiogenic Pb ratio.

(f) Corrected for fractionation, spike, and blank. Also corrected for initial Th/U disequilibrium using radiogenic ^{208}Pb and $\text{Th}/\text{U}_{\text{magma}} = 2.8$.

Mass fractionation correction of $0.18\% \text{ amu}^{-1} \pm 0.04\% \text{ amu}^{-1}$ (atomic mass unit) was applied to single-collector Daly analyses.

All common Pb assumed to be laboratory blank. Total procedural blank less than 0.1 pg for U.

Blank isotopic composition: $^{206}\text{Pb}/^{204}\text{Pb} = 18.15 \pm 0.47$, $^{207}\text{Pb}/^{204}\text{Pb} = 15.30 \pm 0.30$, $^{208}\text{Pb}/^{204}\text{Pb} = 37.11 \pm 0.87$.

Corr. coef. = correlation coefficient.

Ages calculated using the decay constants $\lambda_{238} = 1.55125\text{E-}10$ and $\lambda_{235} = 9.8485\text{E-}10$.